Department of
Mechanical Engineering

Colorado State University

FLAT PLATE ELECTROHYDRODYNAMIC HEAT PIPE EXPERIMENTS

NASA CR-137707

July 1975

by R. I. Loehrke and D. R. Sebits

Mechanical Engineering Department
Colorado State University
Fort Collins, Colorado 80521

NASA Grant #NGR-06-002-127

prepared for
Ames Research Center
National Aeronautics and Space Administration
Moffett Field, California 94035

The work described in this report was performed under NASA Grant NGR-06-002-127, "An Investigation of Electrohydrodynamic (EHD) Heat Pipes." This program is being conducted at Colorado State University with Dr. T. B. Jones and Dr. R. I. Loehrke as principal investigators. The NASA Technical Officer for this grant is Dr. R. J. Debs, NASA Ames Research Center, Moffett Field, California, 94035.

FLAT PLATE ELECTROHYDRODYNAMIC HEAT PIPE EXPERIMENTS

NASA CR-137707

July 1975

by R. I. Loehrke and D. R. Sebits

Mechanical Engineering Department
Colorado State University
Fort Collins, Colorado 80521

NASA Grant #NGR-06-002-127

prepared for
Ames Research Center
National Aeronautics and Space Administration
Moffett Field, California 94035

Contents

I. INTRODUCTION

The theoretical aspects of electrohydrodynamics and its application to heat pipes have been described by Jones in a number of publications.[1,2,3] He proposed using strong, nonuniform electric fields in heat pipes employing dielectric fluids to channel the liquid from the condenser to the evaporator. Axial electrodes maintained at high voltage with respect to the grounded heat pipe case form arteries of low flow resistance which do not depend on capillary forces for their maintenance or priming. These arteries can be coupled with a capillary structure which serves to distribute the liquid over the entire evaporator surface.

The advantages of the electrohydrodynamic (EHD) artery over a conventional capillary driven artery were envisioned to include: positive priming, priming under ebullient conditions, voltage controlled conductance and possibly enhanced heat transfer due to the high electric fields. The power required from the high voltage source under normal operating conditions is extremely small.

The simplest electrode arrangement consists of one or more rods parallel to the pipe axis spaced close to the pipe inner surface. When the rods are charged to a high voltage with respect to the heat pipe shell, the liquid collects in the high field strength regions forming axial tent-like structures, (Figure 1). These tents become open arteries for liquid flow when the heat is added to the evaporator and removed from the condenser. Proof of concept experiments were reported by Jones and Perry[4,5,6] with 3.2 centimeter and 2.5 centimeter outside diameter cylindrical heat pipes each utilizing a single straight wire electrode to form the axial artery. The performance of these pipes was judged to be poor due to a mismatch between the capabilities for axial liquid transport by the EHD structure and the circumferential transport provided by the capillary wicking structure. Evaporator surface regions farthest away from the liquid filled tents dryed out at very low heating rates due the low pumping capacity of the wicking systems. These earliest experiments did demonstrate heat pipe operation and the electrical compatability of the EHD structure with grooved surface and feltmetal capillary systems.

In order to get more detailed information on the performance capabilities and characteristics of an EHD heat pipe, three flat plate heat pipes were constructed and tested. All of these pipes are essentially flattened out versions of the grooved circular heat pipe tested by Jones and Perry. The major features of these heat pipes are displayed in Figure 2. The active surface in each pipe is formed by a flat metal plate with transverse grooves cut in the evaporator and condenser sections. Electrodes are formed by straight axial rods spaced above the active surface. The vapor chamber is closed on the top by a transparent window which allows for observation during operation.

The first version of the flat plate EHD heat pipe was designed primarily to obtain qualitative visual information concerning the priming and performance of the EHD heat pipe. Two copies of this model utilizing

a single axial electrode running down the center of the pipe were constructed and tested with Freon 113 as the working fluid. The third pipe was designed to provide more detailed information concerning the operating characteristics of the EHD heat pipe. Provisions were made in this pipe to vary the number of electrodes and the electrode-to-plate spacing. The third pipe was more fully instrumented with thermocouples than the former and several design deficiences of the former version were eliminated so that evaporator conductance measurements could be made. The working fluid used in the third pipe was Freon 11.

II. SINGLE ELECTRODE FLAT PLATE HEAT PIPE SUMMARY

Two essentially identical flat plate heat pipes were constructed, one of which was tested at the Ames Research Center, the other at Colorado State University. The purpose of these first tests was to visualize the EHD tent during operation and priming and to observe the interaction between the tent and the capillary grooves under load. In these pipes condensation and evaporation occur on opposite ends of a flat brass plate 25.4 cm long and 10.2 cm wide. The plate thickness on the C.S.U. model is 0.32 cm while that on the apparatus tested at NASA is 0.16 cm. The condenser end, 11.4 cm long, is water-cooled from below (constant temperature sink) and the evaporator, also 11.4 cm long, is heated by electric resistance heaters (constant flux source). These two active surfaces are separated by a 2.6 cm long adiabatic section. A 0.16 cm diameter aluminum electrode suspended above the center of the brass plate spans the entire length of the plate from the condenser to the evaporator (axial direction). The gap between the bottom of the electrode and the top of the brass plate is 0.24 cm. The liquid Freon 113 working fluid forms a tent between the brass plate and the electrode when a high voltage (5 to 20 kv for these tests) is applied to the electrode. The grounded brass plate has transverse grooves cut in the surface of the evaporator and condenser to provide capillary liquid transport between the central artery and the uncovered active surfaces. The measured nominal groove profiles are shown in Figure 3. The cover and side walls of the heat pipe are of transparent Plexiglas to facilitate visualization. The vapor chamber formed above the brass plate is 2.54 cm high.

Visualization tests run in these devices demonstrated the heat pipe capabilities of the EHD structure. Operation in adverse gravitational fields (evaporator end elevated up to 1.6 cm above the condenser end), priming under load and control of the amount of evaporator surface wetted in an adverse "g" field are documented in a 16 mm movie. When the electric field is applied with the evaporator end elevated and hot, the tent advances, with increasing applied voltage, over the heated surface and nucleate boiling takes place. This condition is illustrated in the photograph shown in Figure 4. As the evaporator surface is locally cooled under the tents, nucleation subsides and the grooves become wetted. The extent to which the capillary grooves are able to wet the evaporator surface depends upon the elevation of the evaporated surface above the condenser and on the heat load. For zero, or near zero, tilt and with an applied voltage sufficient to prime the entire length of the EHD structure, the entire evaporator surface is covered with liquid when the heat input is zero. As the heat input is increased, the fluid recedes into the capillary grooves. At a heater power of approximately 20 watts, a distinct fluid front in the grooves becomes discernible visually. This fluid front represents groove failure i.e. the furtherest extent of capillary pumping of the liquid on to the evaporator surface away from the EHD tent structure before the liquid supply is exhausted. As the heater power is further increased, this liquid front was observed to recede towards the flow structure. This recession occurs essentially uniformly along the length of the evaporator section. Experimental data are plotted in Figure 5. The difficulty in observing the location of the

liquid front accounts for the uncertainty of the measurements as indicated by the area of brackets on the data. At large tilts the front near the top end of the evaporator moves in further than does that at the lower end of the evaporator forming a tree-like configuration of wetted evaporator surface around the central electrode trunk. Several thermocouples were placed on the lower surface of the brass plate under the condenser and evaporator sections of the heat pipe tested at Ames. The locations of these thermocouples are shown in Figure 6. Two thermocouples were also placed in the vapor chamber to measure the vapor temperature. The temperature excess of the evaporator surface over the vapor temperature as a function of input power is shown in Figure 7. A similar plot showing the difference between condenser temperature and the vapor temperature is shown in Figure 8. The data are in qualitative agreement with the visual observations shown in Figure 5. Evaporator surface dryout is first evidenced by a rise in temperature of the thermocouple most distant from the electrode at a power level of about 15 watts. Due to transverse conduction through the relatively thick brass plate the precise location of the liquid front in the capillary groove cannot be detected by the thermocouple readings. In fact, the liquid tent remained intact along the whole evaporator surface, even up to 50 watts although the thermocouple located under the tent indicated a dryout at about 30 watts. The fact that the condenser conductance in these tests was much lower than the low power evaporator conductance may be attributed to an excess liquid inventory which covered much of the condenser surface with a relatively thick liquid layer.

While the visual and thermal results reported above are in qualitative agreement with predications,[5] quantitative data were not obtainable from these first pipes for several reasons. First, the heat flux distribution over the evaporator on the heat pipe that was run at Ames was not uniform. The evaporator was heated by two strip heaters approximately 5.1 cm by 10.2 cm connected in series and cast in an epoxy plug which fit into a cavity in the Teflon base under the evaporator section. The surface of the epoxy block on which the heaters were mounted is concave, probably a result of shrinkage during the curing of epoxy. Thus when the edges of the heater are in contact with the evaporator plate the center of the heater is about .25 cm away. To eliminate the air space between the heater and the plate the void was filled with a pourable RTV silicon rubber during assembly. With a thermal conductivity of about .21 W/M-°C the RTV is an order of magnitude better than air but still the thermal resistance between the heater and the evaporator plate is higher at the center than at the edges, a situation which tends to force the heat flux to be higher than the average near the edges and lower near the center. Any air which may have been trapped between the plate and the RTV during assembly will further compound the problem and may result in flux nonuniformities not correlated with the curvature of the heater surface. This is probably the cause of the unsymmetrical burnout patterns observed in Figure 7. Another problem is again a mismatch between the axial flow capabilities of the electrode structure and the pumping capabilities of the capillary grooves. With only one axial electrode the grooves were required to pump the liquid from the center of the heated evaporator surface clear out to the edge. This resulted in initial dryout occurring at a very low power level. Furthermore,

in order to achieve the high vapor breakdown field strength required for high tilt operating conditions with Freon 113, the pipe had to be heated considerably above room temperature. For example, with the highest tilt, 1.6 cm, the electrode voltage was 17 kv and the minimum vapor temperature required to prevent electrical breakdown was 38°C. For these high temperatures and correspondingly higher evaporator surface temperatures the heat losses were excessive introducing large uncertainties in the actual heat flux crossing the evaporator surface. For this reason, only low temperature and therefore low tilt data were considered reliable. The relatively thick, 0.32 cm and 0.16 cm, active surface coupled with the short, 2.6 cm, length adiabatic section tended to create relatively high conduction heat losses from the evaporator surface to the condenser surface. These heat losses could only be corrected for approximately. As a consequence of all these problems, the measurements of evaporator and condenser conductances in these first heat pipes was only qualitative. To eliminate some of these problems a second flat plate heat pipe was designed and tested the results of which are reported in the next section.

III. MULTI-ELECTRODE FLAT PLATE HEAT PIPE

This heat pipe is geometrically very similar to the first flat plate heat pipe described in the previous section. The fundamental differences are:

1. The transparent enclosure was made of Lexan, a polycarbonate. This material was reported to be more compatible with Freon 11 than the Plexiglas.[7] Since Freon 11 has a higher vapor pressure than Freon 113 this change in working fluids permits higher voltage and therefore higher tilt operation at room temperature and reduces the nasty problem of trying to minimize and account for the heat losses. This also facilitates viewing the operations since the cover will remain free of condensate.

2. The length of the adiabetic section was increased from 2.5 cm to 10.2 cm to reduce the conduction losses from the evaporator to the condenser. Also the active surface was made of aluminum rather than brass of a thickness of 0.8 mm. The same forming tool was used for cutting the grooves in this surface as was used in the two previous flat brass plates.

3. The grooved plate, heating element foil and Lexan base plate were cemented together. This eliminated the buckling of the groove plate under conditions of negative internal pressures and provided intimate uniform contact between the evaporator surface and heater foil.

4. The heat pipe was designed to accommodate multi-electrodes. Basic design was for 3 parallel axial electrodes and subsequent modifications enabled the use of 6 parallel axial electrodes. Also, provisions were made so that the electrode-plate spacing could be easily varied. Detailed description of the construction and experimental procedures is presented in the next section.

A. Apparatus

The heat pipe was constructed from three 1.27 cm thick Lexan sheets and one 0.8 mm thick aluminum plate. The Lexan sheets formed the cover plate, base plate and the vapor chamber side walls. The aluminum plate formed the active surface of the heat pipe. The details of these four components are shown in Figures 9 - 12. The cover plate and cell were glued together to form a cap which defined the top and sides of the vapor chamber. Capillary grooves were machined into the top surface of the aluminum plate over the evaporator and condenser sections only. An ungrooved adiabatic section of the plate was located between the grooved areas. The grooves were 7.62 cm long and approximately .13 mm in width with a density of 39.4 grooves per cm. The groove dimensions and shape were determined by pouring liquid silicone rubber (RTV) onto the grooved areas and allowing it to harden. After hardening, the molded RTV was

pulled away from the grooved surface, sectioned and photographed with a metallurgical microscope. (See Figure 13.) The Lexan base plate was machined to provide a recess for the electrical heater on the evaporator end and water cooling channels on the condenser end. A .64 cm thick aluminum plate was machined to form a cap for the water cooling channels. Twenty eight, 36 gage copper-constantan, thermocouples were bonded to the lower surface of the grooved aluminum plate with epoxy. The locations of these beads is shown in Figure 14.

A base plate subassembly was then formed by glueing together, with a silicon rubber adhesive, the instrumented aluminum active surface, the aluminum cooling channel cover plate, a Minco HK 6070-03A8.25 thin film electrical resistance heater and the Lexan base plate. The insulated thermocouple leads emerged from the side of this sandwich. The diameter of these leads, 0.18 mm, is a measure of the spacing between the lower surface of the aluminum plate and the upper surfaces of the heater and cooling channel cover plate. The reason for glueing this subassembly together was to support the thin aluminum plate under conditions of low internal vapor chamber pressures.

To form the heat pipe the base plate assembly and the cap assembly were bolted together. (Figure 15). Three electrodes emerged from the vapor chamber through grooves machines in the lower surface of the vapor chamber side walls. These apertures were sealed during assembly with RTV. The thickness of the Teflon gasket defined the electrode to plate spacing.

The electrodes were made of 1.6 mm diameter aluminum welding rod. The design configuration for the heat pipe utilized three electrodes with a spacing of 2.54 cm between electrode centers. Since the heat pipe top cover had provisions (machined grooves) for only three electrodes, a special adapter was required to provide six electrode capabilities while leaving the top cover unmodified. The six electrodes were made of 1.6 mm diameter aluminum welding rod and were attached to Lexan mounting blocks (Figure 16.) Tension in, and support for the electrodes was provided by three threaded aluminum studs in each Lexan block. The studs were located in the block to match the three machined grooves in the top cover. Electrical connection between the six electrodes and one support stud was provided by a fine copper wire connecting the electrode set screws in the Lexan block.

Two apertures were drilled through the side of the vapor chamber. One near the adiabatic section held a Swagelock fitting through which passed a sheathed copper-constantan thermocouple for vapor temperature measurements. The other, at the condenser end, held a valve which was used for filling and venting.

The entire heat pipe assembly was mounted on a rectangular Plexiglas frame to which 28 thermocouple connecters were bonded. The frame was attached to a supporting base with provision for varying the tilt angle of the heat pipe with respect to a horizontal reference.

Electrode to base potential difference was maintained with a high voltage direct current power supply (0-15 K.V. Beta Electronics 1015-5). Current was supplied to the resistance heating element by connecting two variacs (variable voltage autotransformers) in series to better the impedance match between the heater and the transformer. Power flow to the heater was determined by taking voltage and current measurements within the heater circuit. Cooling water was supplied to the heat pipe condenser section by immersing a submersible pump (Little Giant 2E38N) into a five gallon reservoir. The reservoir was used to smooth slight variations in the flow rate and temperature of water from a temperature controlled mixing valve. Thermocouple voltages were recorded by a 12 channel Leeds and Northrup (Model 66-41586-1-1) millivoltmeter.

B. Procedure

Prior to running a conductance test, the heat pipe base plate was thoroughly cleaned with F-11 (or F-113) to purge foreign material from the capillary grooves. After cleaning, the heat pipe was assembled and partially filled with 10-15 ml of Freon-11. To remove the entrapped air the heat pipe was tilted such that the Freon filler port was at a higher level than the chamber and the greater density of the Freon forced the air into a pocket surrounding the port. Since the vapor pressure of Freon-11 is above atmospheric pressure at room temperature, the entrapped air was forced from the chamber when the filler port valve was opened. The desired tilt angle of the base plate was then set by leveling the supporting frame and measuring the vertical distance from two points on the base plate to a horizontal reference plane.

To initiate a test, the electrode potential was slowly raised to approximately 90% of the calculated vapor breakdown voltage. The evaporator wetting process was observed while increasing the electrode voltage and if no arcing occurred and if the liquid tent covered the full length of the evaporator a heat load was applied. Before a set of temperature data was recorded the heat load was maintained at a constant level for approximately 45 minutes to insure thermal equilibrium throughout the heat pipe. After a set of data was taken the heat load was usually increased in equal power steps and a set of temperature data was taken at each step. Condenser cooling water was maintained at approximately 16°C throughout all tests. A test run was terminated for one of two reasons; either extensive dryout of the evaporator surface caused excessively high surface temperatures or the vapor pressure in the chamber reached an upper limit. A vapor temperature of 54°C corresponding to a pressure of about 2.5 atm was that limit.

The heat pipe was operated in two, three and six electrode configurations with electrode to base plate gap spacings of .5 and 1 mm. All two electrode test runs were made with base plate tilt angles of 1.95° and 3.73° and a .5 mm electrode gap spacing. In order to increase

the gap spacing to 1 mm, the previously mentioned .5 mm gasket was replaced by a thicker 1 mm gasket. A calculated value of 9 KV was to be the 1 mm gap operating voltage, however electrode to plate arcing began in air (external to the heat pipe chamber) at about 5 KV. The problem was remedied by sealing all external electrode to plate air gaps with RTV-60 (General Electric Silicon Rubber Compound). High heat load test runs were made with a cautious eye on vapor temperature and the accompany high internal pressure since evaporator dryout temperature was elevated over the .5 mm gap runs. The maximum base plate tilt angle at which complete evaporator wetting could be accomplished with the 1 mm gap and 9 KV was approximately 6°. Since operation at the 6° tilt angle would have resulted in very low power evaporator dryout the angles chosen for test runs were 5°, 4° and 3°.

The physical configuration for two electrode operation was identical to that for three electrode operation but in the two electrode mode the center rod was grounded so that liquid tents were formed only around the two off-center rods. In order to operate the heat pipe in its six electrode mode, the special six wire adapter was constructed and fitted to the chamber. The 1 mm gasket was used since the .5 mm gasket did not provide adequate clearance between the adapter supporting frame and the heat pipe base plate. An unfortunate problem with the six wire adapter was the inability of the three threaded studs to provide adequate tension in the six electrodes. Tension in the electrodes is required due to the electric field force attracting the electrodes to the base plate. When a voltage of approximately 5 KV was applied to the six electrodes, they began vibrating in a transverse mode which would intermittently close the electrode to base spacing enough to cause arcing. To prevent the vibration, a 7.7 cm long, 2 mm wide section of 1 mm thick Teflon gasket was placed under the electrodes at midspan. The resulting support allowed electrode potentials of 9 KV to be used during test runs. A single run at 3.35° base plate tilt angle revealed a partial restriction of the EHD flow structure and further runs at high heat load and high tilt angle were deleted. The electrode support was apparently responsible for the restriction.

In order to provide adequate working fluid to the evaporator, the condenser was necessarily operated in a flooded (thick fluid layer) condition. As a result the condenser conductance was generally lower than the evaporator conductance and was very sensitive to tilt and total fluid inventory. Due to the difficulty in characterizing the condenser conditions for these tests the measurements were focused on evaporator performance.

After a set of test runs had been completed, the accumulated data was reduced in the following manner. Temperature values at specific points on the base plate surface were calculated from the recording millivoltmeter data. The actual temperature at a given location was not of considerable interest since conductance values are based on temperature differences between the evaporator surface and the vapor. One method of

calculating evaporator conductance was to consider the temperatures of the thermocouple location points individually as follows.

$$U_{evap_i} = \frac{\text{Heat Load}}{T_i - T_{vapor}}$$

The equation yields an area dependent conductance at some i^{th} location based on the i^{th} Δ Temperature. Numerical values for use in this equation were extracted from graphs of evaporator ΔT plotted against heat load. Another method was to calculate a mean value for evaporator ΔT at each heat load level for a particular test. The average ΔT's were then plotted against input power level (heat load) and a slope could then be extracted from the linear portion of the graph. The slope of the plotted line is the inverse of the average evaporator conductance.

$$\text{Slope} = \frac{\overline{\Delta T^E}_{\text{upper power level}} - \overline{\Delta T^E}_{\text{lower power level}}}{(\text{upper power level}) - (\text{lower power level})} = \frac{1}{\overline{U}_{evap}}$$

The heat load level at which initial evaporator dryout began could be determined in two ways. One method was to visually observe the evaporator surface, however the location of the fluid front was not always obvious and the reliability of this method was questionable. The procedure actually used during most test runs was to increase the heat load to a level at which a large percentage of the evaporator surface was dry and then plot evaporator ΔT vs. heat load. Large scale evaporator dryout could always be determined by a sharp increase in average evaporator temperature with only a small increase in heat load. The evaporator ΔT vs. heat load plots were carried out to the maximum power level for a given test to insure the inclusion of the initial dryout point within the plot.

C. Results

Qualitatively, the performance of this heat pipe using Freon 11 with two and three electrodes at .5 and 1.0 mm spacings was identical to the earlier flat plate pipes. Heat loads were never high enough to dry out the evaporator surface under the tents. In all cases the heat load was limited either by the internal vapor pressure limit or by excessive evaporator surface temperature caused by between-tent dryout. In contrast, in the six-electrode configuration tent dryout was observed at relatively low heat load. This was attributed to the extra flow resistance provided by the Teflon support block required for six-electrode operation as described in the previous section. In spite of the deleterious effect of this added resistance on the dryout heat load sufficient liquid flow could be achieved at low power to assess the effect of the additional electrodes on evaporator conductance.

Calibration Test

Preliminary EHD tests with two and three electrodes indicated evaporator surface temperature variations which appeared uncorrelated with variations in the liquid film thickness. In order to evaluate the contribution of the apparatus and instrumentation to these observed non-uniformities a calibration test was run with a nominally uniform evaporator surface conductance. For this test the electrodes were removed and the heat pipe was operated in a horizontal position with a deep (approximately 2 mm) liquid layer over the entire active surface. The axial variation in the liquid layer thickness and temperature associated with the return flow from the condenser was negligible at low power levels so that the evaporator was blanketed by an essentially uniform conductance layer. Under these conditions all of the evaporator surface thermocouples should have indicated identical temperatures at a given power level. Possible variations in the liquid layer conductance due to cellular convection were of sufficiently small scale and magnitude to be immeasurable as temperature variations in the .8 mm thick aluminum plate. Never-the-less measureable evaporator surface temperature variations were observed. The results of this test are presented in Figures 17 through 19. The cause of the approximately ±25% variation in surface temperature excess under these nominally uniform conductance conditions must be associated with thermocouple attachment inhomogeneities. Although the flattened thermocouple beads were carefully pressed in contact with the aluminum plate prior to being covered with epoxy a continuity check after assembly revealed that fewer than half of the thermocouples were in electrical contact with the plate. On the evaporator surface only thermocouples 1, 6, 8, 13, 14 and 16 are in contact. Thermocouple 15 did not survive the assembly intact. The thermocouple mounting errors are further compounded by inhomogeneities in the heater construction. The Minco heater is formed by encapsulating a metallic resistance grid in a Kapton film. Although the resulting non-uniformities in heat flux are smoothed out in the aluminum plate, thermocouples not in intimate contact with the plate can be strongly biased by the heater geometry. Since rectifying this problem was tantamount to constructing a new base plate assembly it was decided to continue the testing program with the existing apparatus. An attempt was made to use the results of this calibration test to correct the temperatures measured in the EHD operation to try to detect variations in liquid film conductance associated with the electrode-tent geometry.[8] Unfortunately, no simple model for the thermocouple errors in the uniform conductance tests was found which would yield local conductance variations in the EHD test consistent with geometrical symmetries. As a consequence only average evaporator conductance data are reported here. The average conductance is based on the average of 15 evaporator surface temperatures. Thermocouples 1, 7 and 9 which are located near the edges of the heated evaporator surface and are most strongly influenced by side-wall conduction losses were not included in the average.

EHD Tests

A typical set of evaporator surface temperature data is shown in Figure 20. Although the variation among individual thermocouple readings is large the slopes are relatively constant up to a power level of about 20 watts. Above this power level the slopes increase noticeably indicating partial surface dryout. An extrapolation of these data back to zero input power yields a positive value for ΔT. This apparent anomaly prompted a further investigation of the surface temperature variation at low input power the results of which are presented in Figure 21. A dramatic increase in conductance occurs in the input power region between 0 and 5 watts. Above 5 watts the conductance remains relatively constant up to initiation of dryout. This sort of behavior has been observed in other grooved surface heat pipe experiments and is discussed in Reference 9, p. 197. This effect appears to be a strong function of groove shape and surface geometry. In most of the experiments reported here the average conductance at power levels above about 5 watts remained relatively constant up to dryout. In all cases the reported average conductance is based on the average surface temperature rise between the two lowest power levels at which data were taken above 5 watts.

The average conductance measured in this manner for all of the experimental configurations tested are presented in Table I. Included are data for 2, 3 and 6 electrode operation with 0.5 mm and 1.0 mm spacing between the electrode and the plate. For all runs the electrode potential was set at a value just below that which would result in breakdown in the vapor chamber. Over this whole range of geometries and tilts the measured conductance ranged from 0.063 to 0.149 watt/cm^2-°C. The lowest value was found for the two electrode configuration at high tilt and may be spurious. No definite break point in the temperature-power curve could be detected for this run indicating that partial dryout occurred at a power level below the lowest values used to define conductance.

Plots of average evaporator surface temperature versus input power for the different electrode configurations are shown in Figures 22 through 24. The absence of a well defined breakpoint associated with surface dryout for two-electrode operation is evident when contrasted with the three electrode results as in Figure 22. As expected the dryout power level decreases with increasing tilt for a given electrode geometry. The effect of increasing the electrode to plate spacing can be seen by comparing the 3 electrode, 0.5 mm gap results in Figure 22 with the 3 electrode, 1.0 mm data in Figure 23 The reduction in liquid flow resistance accompanying the increase in gap pushes the dryout heat load at a given tilt to a higher level. In fact, at the lower tilts for the 1.0 mm gap the heat flux and associated superheat become so high that nucleate boiling was observed in the EHD flow channels. This condition was observed for the 3° and 4° tilts (Figure 23) at power levels above 50 watts and, together with transverse conduction in the aluminum plate, accounts for the suppression of dryout and increase in average conductance noted for these two runs at about the same power level. Nucleate boiling under the electrodes was not observed in any runs with 0.5 mm gap.

Finally, the six electrode results are shown in Figure 24. As noted previously dryout for the six electrode test was accompanied by starvation of the EHD tents due to the flow restriction imposed by the required electrode support spacers. Thus the low dryout level indicated in Figure 24 is not directly comparable with the data from the two and three electrode tests.

D. Discussion of Results

The average conductance for all of the three and six electrode runs shown in Table 1 is 0.103 w/cm^2-°C. Because of the thermocouple attachment variations the values reported here are actually low estimates of the film conductance. There is some indication that the conductances with a 0.5 mm gap are higher than those with a 1 mm gap however one must be careful not to over-interpret this data. Partial dryout of the evaporator surface due to differences in tilt and liquid inventory from run to run could influence the measured conductance. A negligible change in average conductance was observed when the number of electrodes was increased from three to six. This outcome is consistent with the results of a simplified thermal analysis of the evaporator. A two-dimensional conduction model of the evaporator surface was constructed assuming uniform heat flux input from below and a variable thickness liquid layer above with the liquid free surface maintained at the vapor temperature. The liquid layer was thick near the electrodes and shaped to approximate the EHD tent. Between tents the liquid layer was uniform in thickness. The thickness of this uniform layer was adjusted to match the measured average conductance for the three electrode configuration and the change in average conductance was then calculated when the number of tents was doubled with this same between tent film thickness. The results indicated that doubling the number of insulating tents from three to six should decrease the average conductance by only 5%. Clearly, even with six electrodes equally spaced over the evaporator section the heat transfer processes in the uncovered grooved areas still set the average conductance. With this in mind an estimate of the evaporator conductance was made using the design equations proposed by Feldman and Berger.[9] For this purpose the groove profile shown in Figure 13 was idealized as a rectangular groove, 0.076 mm deep, 0.127 mm wide with a density of 39.4 grooves/cm. From design equation (4.11) of Reference 9 with Freon 11 liquid properties one obtains an estimate of 0.32 w/cm^2-°C for the evaporator conductance. This is a rather substantial overestimate of the measured performance and points up the need for improved experimental data. All of the dryout data are consistent with intuition. For a fixed electric field strength the dryout heat level increases with the number of electrodes and decreases with increasing tilt. Also, the burnout heat load was substantially higher with the 1.0 mm gap than with the 0.5 mm gap. So much so in fact that nucleate boiling was observed under the thicker EHD tents. The onset of nucleate boiling was correlated with an increase in average evaporator conductance and in the 4 degree tilt run shown in Figure 23 actually appears to have suppressed the effects of local surface dryout.

IV. SUMMARY AND CONCLUSIONS

Experiments with three different flat plate EHD heat pipes have been performed utilizing Freon-113 and Freon-11 as a working fluid. All of these pipes employed straight rod electrodes to form axial liquid flow channels and transverse grooves for capillary surface wetting. The following conclusions are drawn from the results of these experiments:

1. The EHD heat pipe will prime under load. Vapor bubbles formed in the axial liquid channels are readily expelled and the capillary grooves become wetted as the local surface temperature drops below the nucleation point.

2. Voltage controlled conductance can be achieved by varying the active area of the evaporator. The heat pipe operation is stable with the axial flow structure partially covering the evaporator surface. With the electrode geometry used in these flat plate pipes conductance control in a gravitational field can only be achieved with the evaporator end elevated above the condenser end. With the addition of a separately controlled reservoir electrode in the condenser section it should be possible to control the liquid inventory so that variable conductance can be obtained with either end elevated.

3. The average evaporator conductances measured in these experiments were consistent with those obtained in other experiments with heat pipes of similar surface geometry using the same or similar working fluids.[10,11] The measured conductance, based on the average evaporator surface temperature, increased sharply as the input power was increased from zero to approximately 5 watts. Above 5 watts the conductance, for a given electrode configuration, remained relatively constant with increasing power until either local surface dryout occurred or nucleate boiling began in the electrode flow structure. In the constant region the conductances ranged from 0.07 w/cm^2-°C to 0.149 w/cm^2-°C for different runs. The onset of nucleate boiling was accompanied by an increase in average conductance.

Although uncertainties associated with the surface thermocouple instrumentation preclude any definitive statements concerning the absolute level of the evaporator conductance several qualitative conclusions can be drawn. Over the range of electrode configurations tested (2 to 6 parallel electrodes at 0.5 mm and 1 mm plate to electrode spacings) the major effect of electrode geometry changes was on the dryout power level. Slightly higher conductances were measured with the 0.5 mm gap than with the 1 mm gap but aside from that no definite correlation was observed between electrode geometry or tilt and conductance. The dryout power level at a given tilt increased with increasing gap and number of parallel electrodes for the two and three electrode configurations. The addition of a short spacer block between the electrodes and plate in the six electrode configuration caused a severe flow restriction which resulted in a dryout level lower than that in the three electrode configuration. The conductances for the two cases were, however, nearly identical. The implication

of these observations is that for low power operation the use of solid, insulating standoffs between the electrodes and active surfaces may be perfectly acceptable but that for high power capabilities every effort must be made to avoid blocking the liquid return area.

V. RECOMMENDATIONS FOR FUTURE WORK

Among the unanswered questions concerning the EHD heat pipe performance the most basic are concerned with the interaction of the electrode-liquid flow structure and the active heat transfer surfaces. To what extent do the thick liquid tents degrade the conductance of the evaporator and condenser surface? In other words, what is the trade-off, if any, between average conductance and axial flow structure density? Are the transverse grooves really necessary or can a successful pipe be constructed with closely packed electrodes over smooth active surfaces? Is electroconvection, or some other convection mechanism, important for heat transport in the liquid tents? Is it desirable to design a heat pipe so that the evaporator normally operates in the nucleate boiling regime?

In order to answer any of these questions it is necessary to be able to accurately measure the surface temperatures in the evaporator and condenser. Ideally, one would like to be able to measure local values of surface conductance and correlate these with the surface geometry and with visual observations. To do this would require a rather sophisticated experiment in which local values of surface temperature and heat flux could be determined. In order to gain some insight into the phenomena and to answer some of the questions in a global sense a simpler experiment has been designed. In this experiment thick brass plates will be used for the active surfaces. Transverse conduction in these plates will provide for uniform temperature surfaces in both the evaporator and condenser. Thermocouples will be imbedded in the plates to accurately determine the surface temperature levels. Total power input will be measured to determine the average surface heat flux and from these temperature and heat flux measurements average surface conductances will be defined. Both grooved and ungrooved surfaces will be studied. The grooved surfaces will be salvaged from the single electrode heat pipe apparatus described earlier in this report and modified to reduce conduction transport between the evaporator and condenser ends of the pipe. Straight axial electrodes will again be used. The electrode support structure has been designed so that the 0.16 cm electrodes can be spaced on 0.32 cm centers or any multiple of 0.32 cm. The electrode to plate gap can also be varied so that operation with overlapping tents will be possible. Finally, a reservoir has been provided on the condenser end of the heat pipe so that excess liquid inventory will not flood the condenser surface and degrade its performance.

With this apparatus quantitative information concerning the influence of electrode-surface parameters on average evaporator and condenser conductance will be obtained. From the outcome of these experiments one can then judge whether or not more detailed, local conductance measurements are warrented.

References

1. Jones, T. B. and Melcher, J. R., "Dynamics of Electromechanical Flow Structures," Phys. of Fluids, Vol. 16, No. 3, p. 393, 1973.

2. Jones, T. B., "The Feasibility of Electrohydrodynamic Heat Pipes," Research Report No. 1, Colorado State University, NASA CR-114392, Oct. 1971.

3. Jones, T. B., "An Electrohydrodynamic Heat Pipe," Mechanical Engineering, p. 27, Jan. 1974.

4. Jones, T. B. and Perry, M. P., "Experiments with an Electrohydrodynamic Heat Pipe," Research Report No. 3, Colorado State University, NASA CR-114498, Sept. 1972.

5. Jones, T. B. and Perry, M. P., "Electrohydrodynamic Heat Pipe Research," Research Report No. 4, Colorado State University, NASA CR-114646, July 1973.

6. Jones, T. B. and Perry, M. P., "Electrohydrodynamic Heat Pipe Experiments," J. of Applied Physics, Vol. 45, No. 5, p. 2129, May 1974.

7. "Freon MF Solvent," Bulletin No. FST-7A, Freon Products Division, E. I. du Pont de Nemours and Co., Wilmington, Delaware, Feb. 1973.

8. Sebits, D. R., "Evaporator Conductance and Dryout in an Electrohydrodynamic Heat Pipe," M.S. Thesis, Colorado State University, Jan. 1975.

9. Feldman, K. T., Jr. and Berger, M.E., "Analysis of a High-Heat-Flux Water Heat Pipe Evaporator," Technical Report ME-62 (73) ONR-012-2, The University of New Mexico, Sept. 1973.

10. Loehrke, R. I. and Debs, R. J., "Measurements of the Performance of an Electrohydrodynamic Heat Pipe," AIAA paper 75-659, AIAA 10th Thermophysics Conference, May 1975.

11. Kosowski, N. and Kosson, R., "Experimental Performance of Grooved Heat Pipes at Moderate Temperatures," Fundamentals of Spacecraft Thermal Design, John W. Lucas, ed., Vol. 29 of Progress in Astronautics and Aeronautics, p. 417, 1972.

Test Run (date)	# of Electrodes and Gap Spacing	Tilt Angle (degrees)	Average Conductance (watt/cm^2 C)	Electrode Voltage (Kvolts)	Cooling Water Temp. (C)
4/25/74	3-.5mm gap	2.87	0.116	4.5	18.3
5/5/74	3-.5mm gap	3.73	0.149	4.5	15.6
5/14/74	2-.5mm gap	3.73	0.063	4.5	12.8
5/26/74	2-.5mm gap	1.95	0.105	4.5	12.8
10/7/74	6- 1mm gap	3.35	0.100	9.0	15.6
10/13/74	3- 1mm gap	5.00	0.070	9.0	15.6
10/10/74	3- 1mm gap	4.00	0.090	9.0	15.6
10/14/74	3- 1mm gap	3.00	0.095	9.0	15.6

Table 1. Variable parameter data and average evaporator conductances

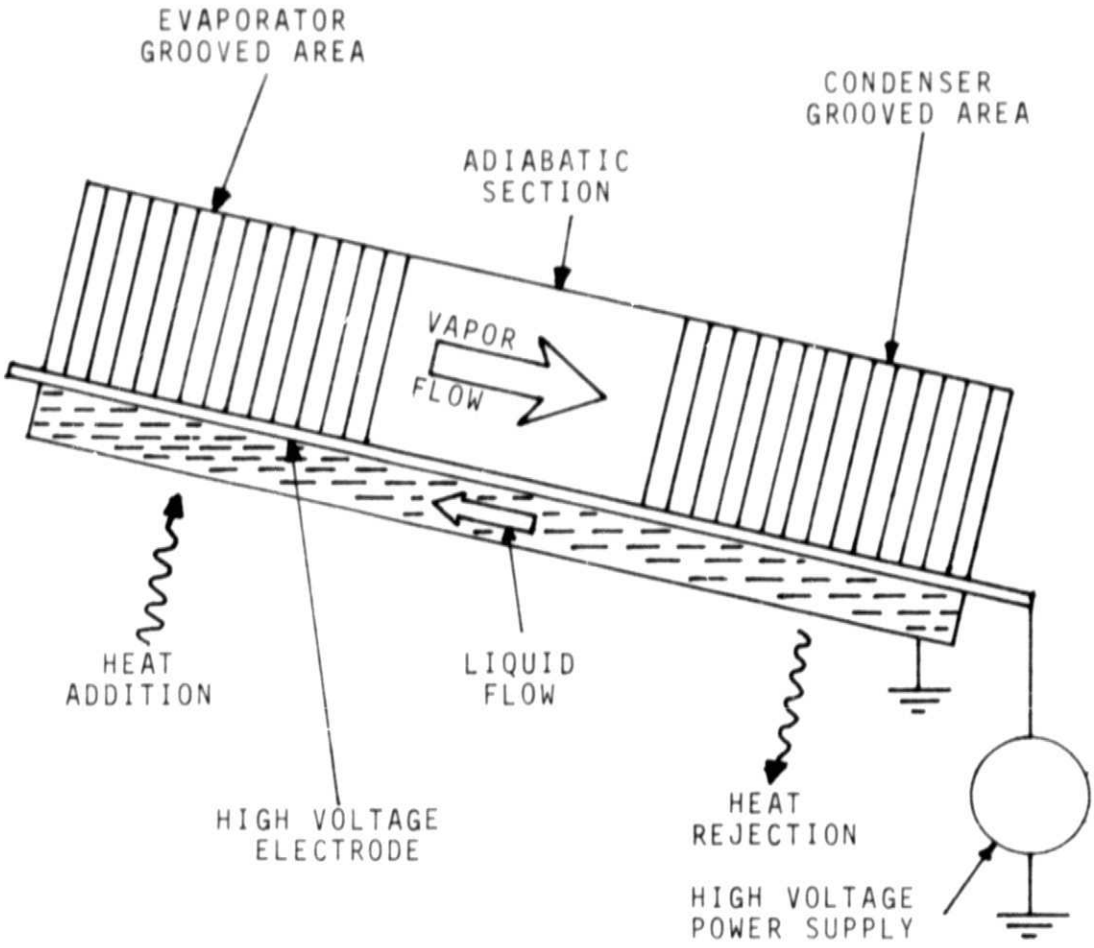

SECTION AA

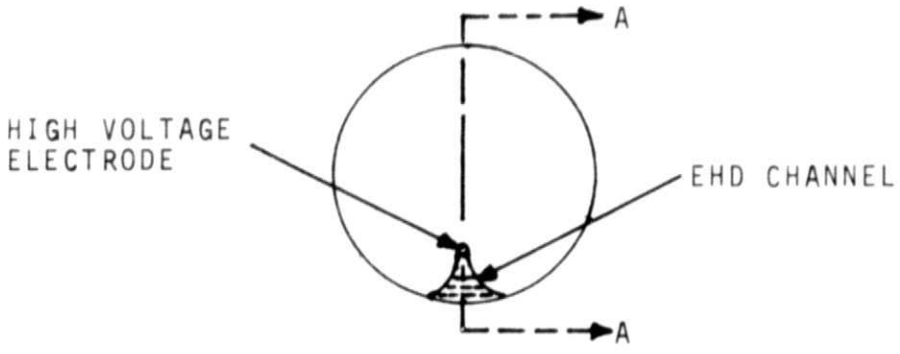

Figure 1. Schematic of an EHD Hea Pipe.

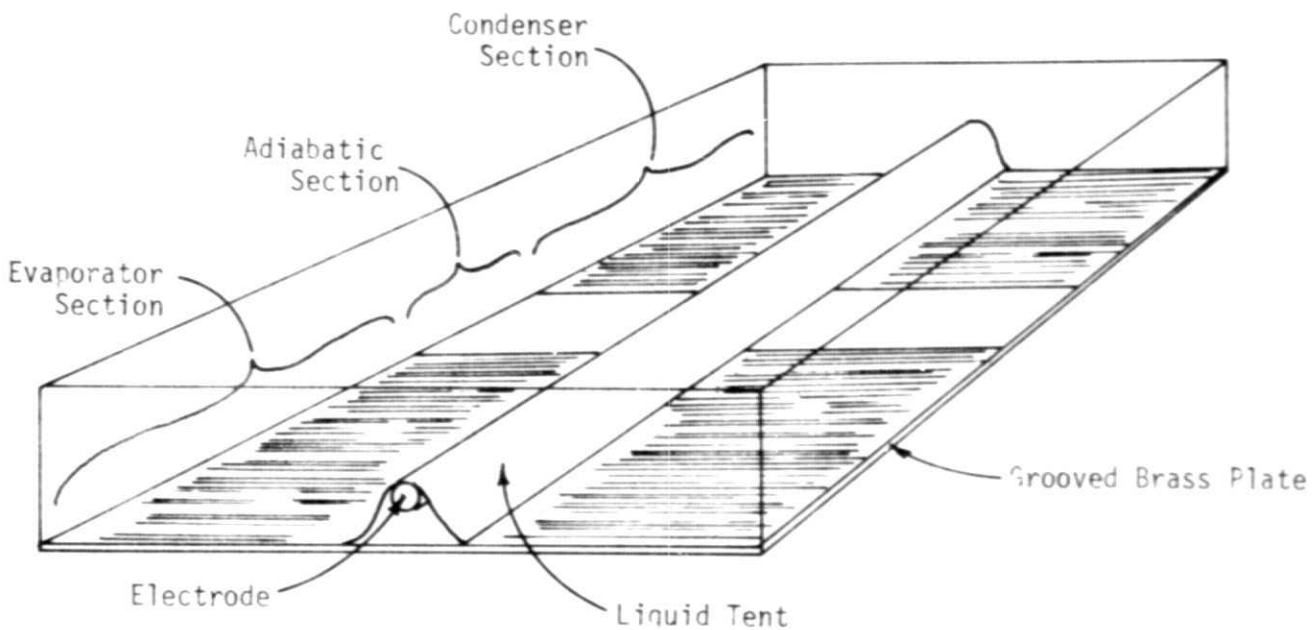

Figure 2. EHD Flat Plate Heat Pipe

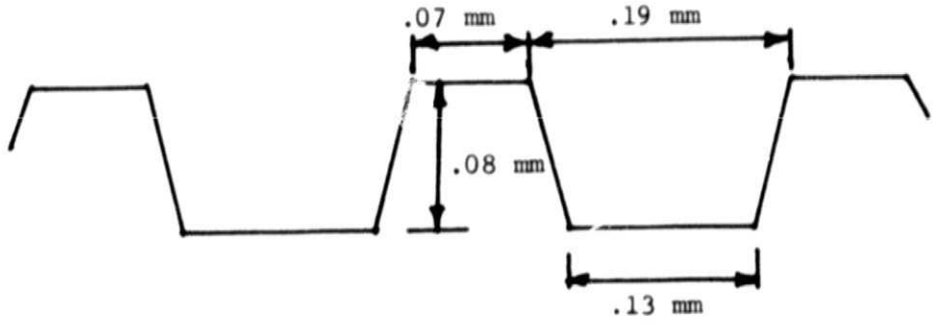

Figure 3. Detail of Groove Cross Section.

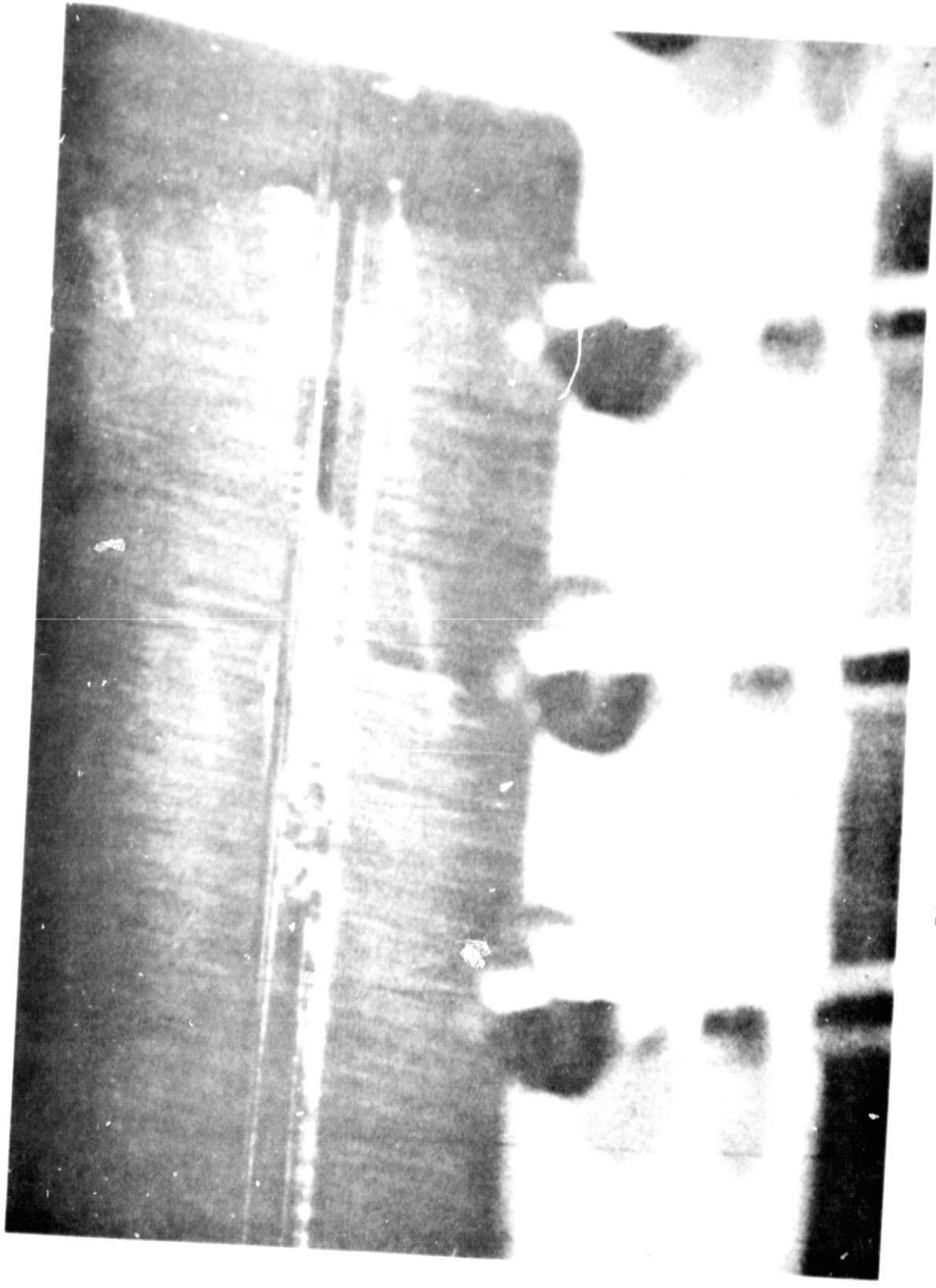

Figure 4. Evaporator Priming Under Load.

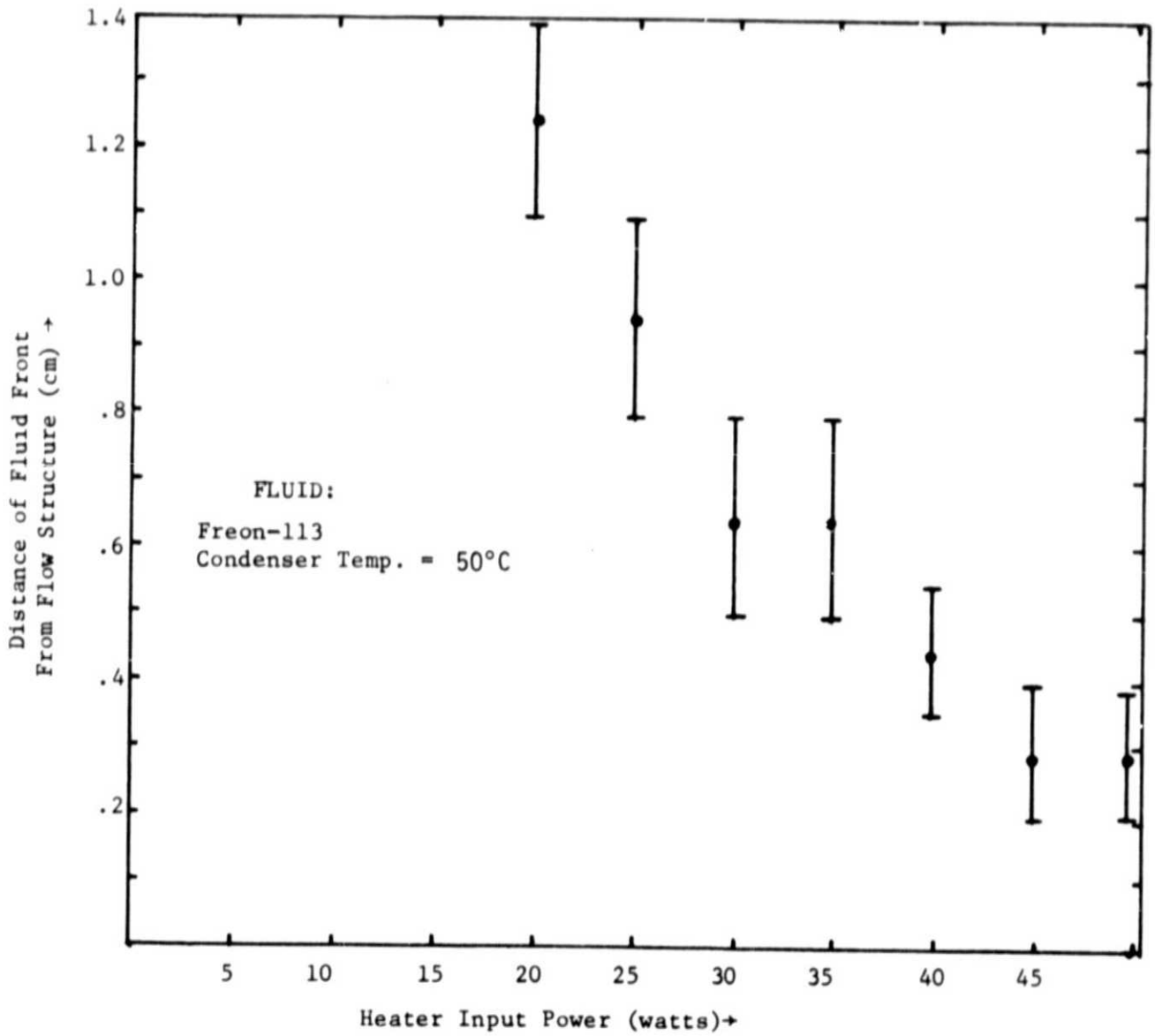

Figure 5. Experimental Data Showing Fluid Front Location versus Heater Input Power at Low Tilt

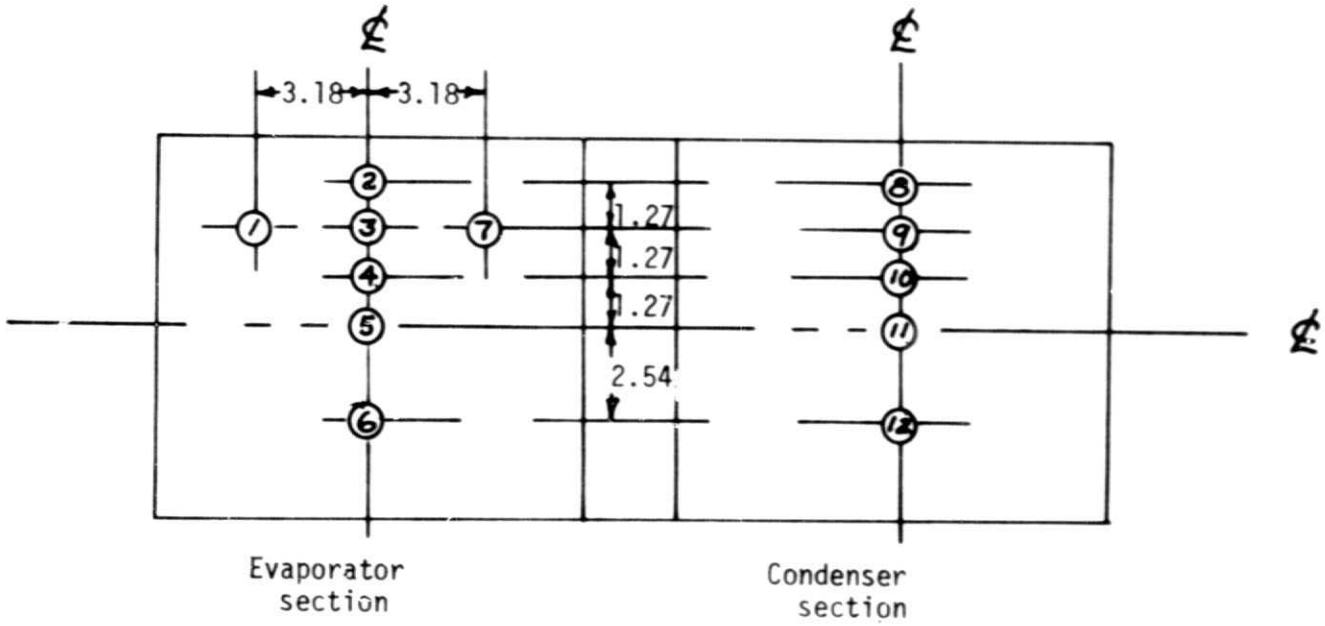

Figure 6. Thermocouple Locations. Dimensions in Centimeters.

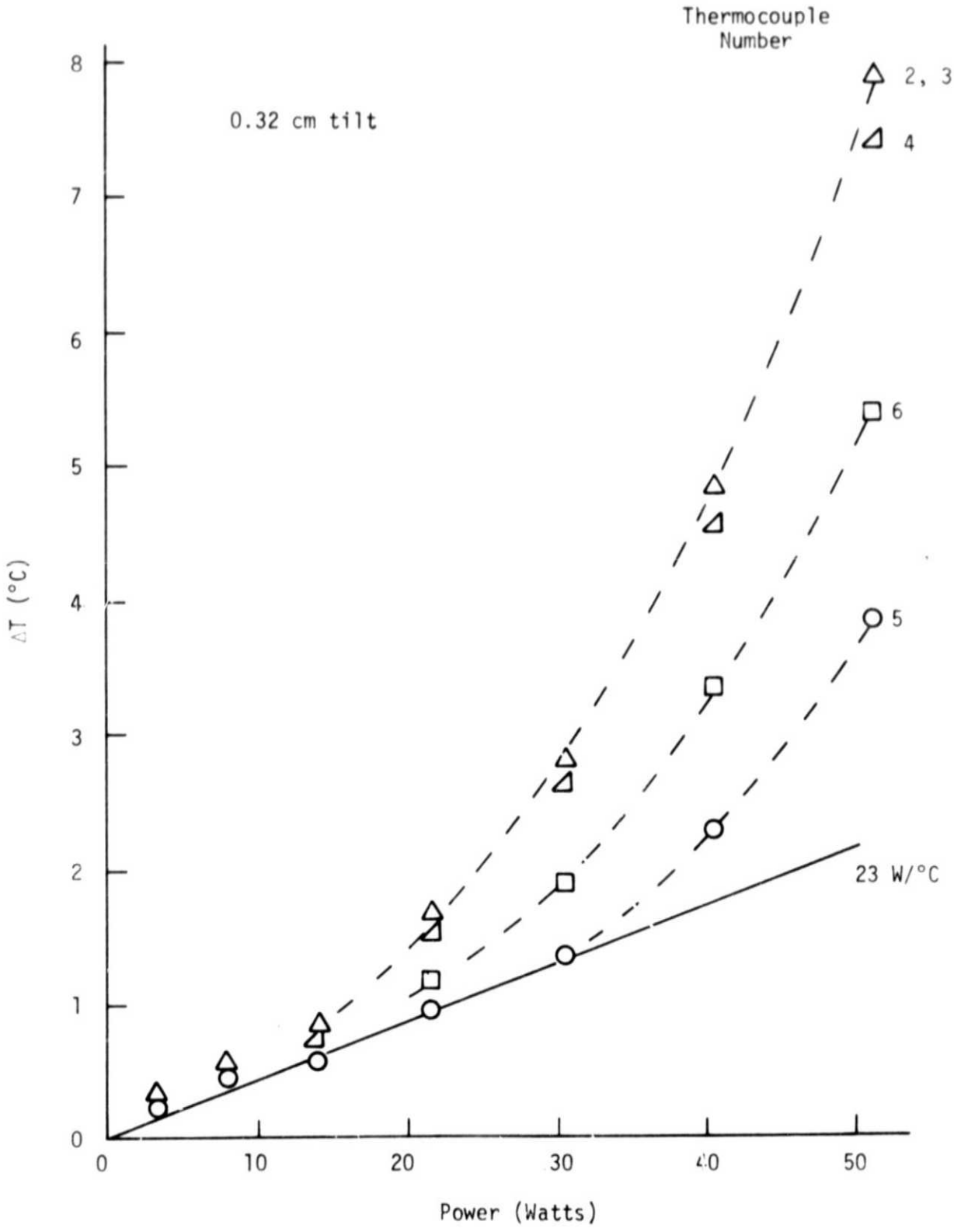

Figure 7. Evaporator Surface Temperature Superheat versus Power.

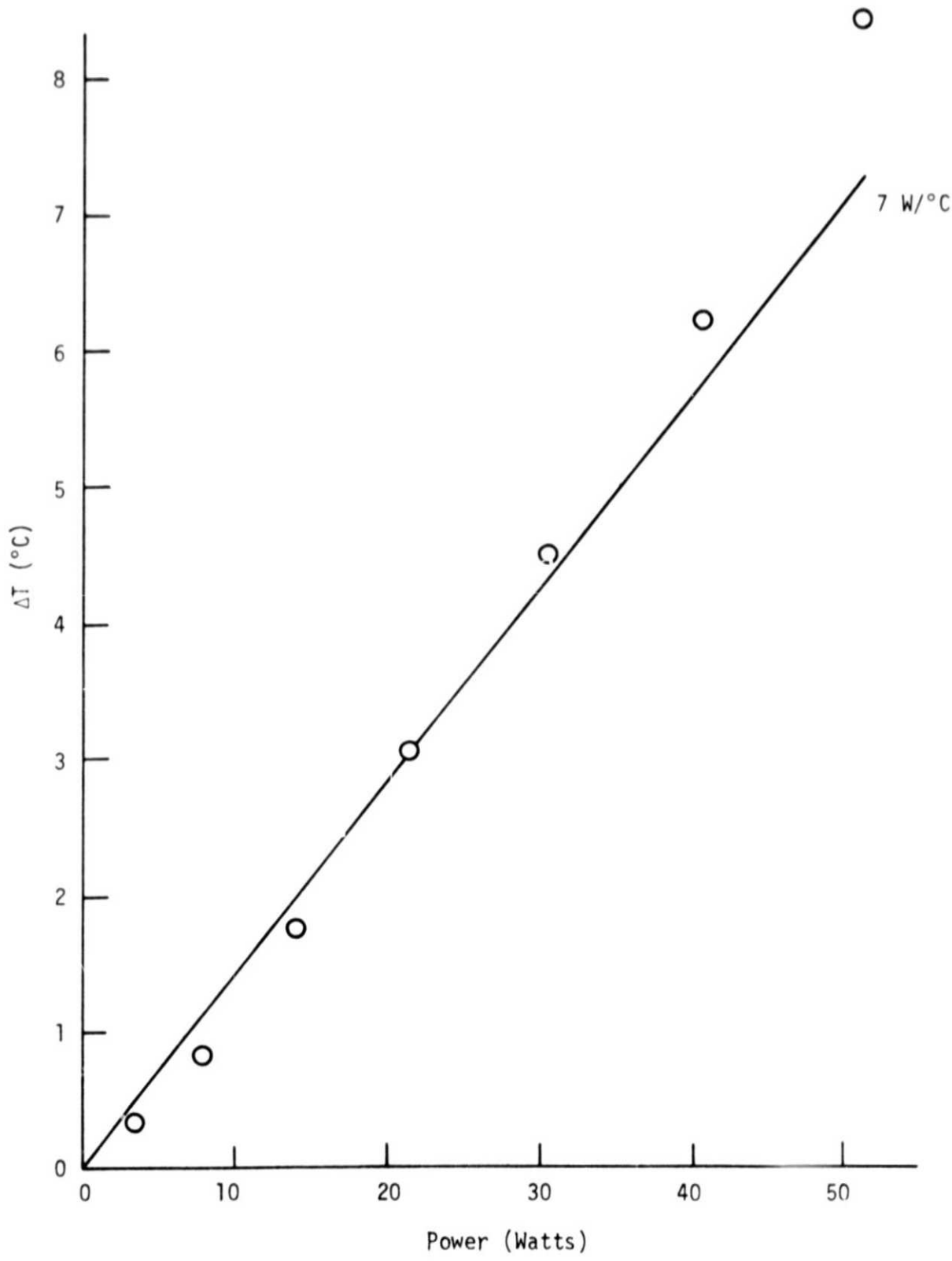

Figure 8. Condenser Surface Temperature Subcooling versus Power.

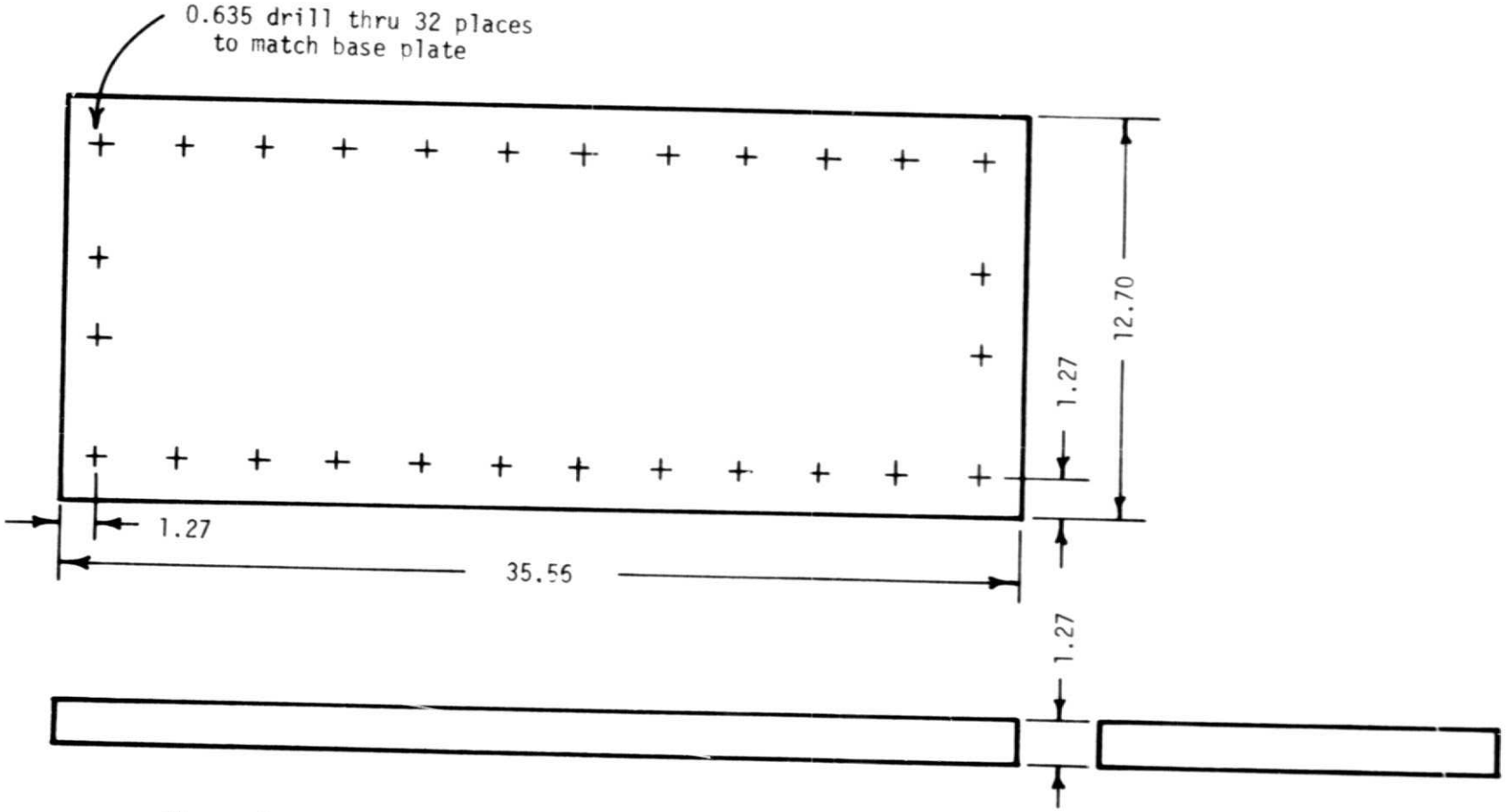

Figure 9. Lexan Cover Plate. Dimensions in Centimeters.

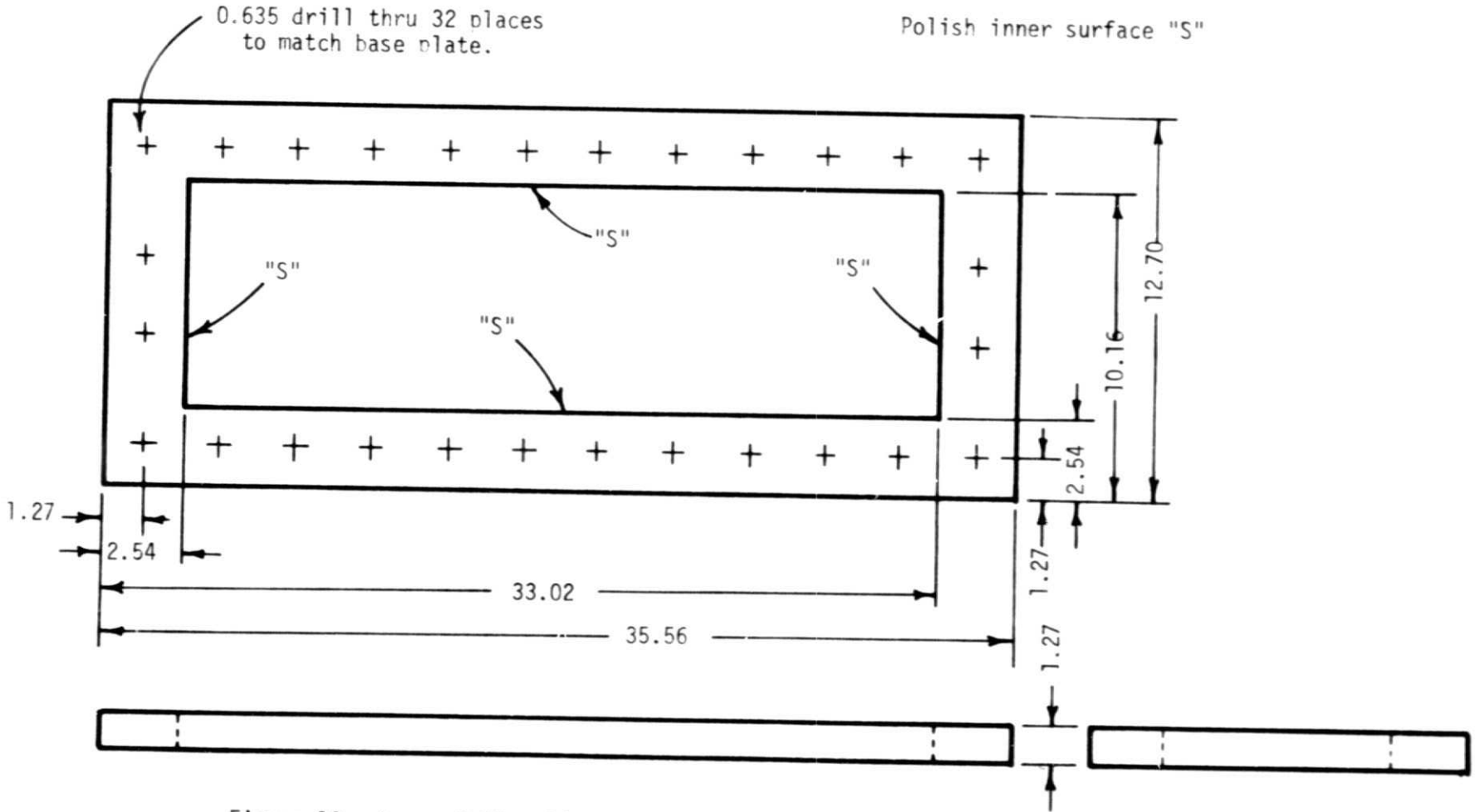

Figure 10. Lexan Cell. Dimensions in Centimeters.

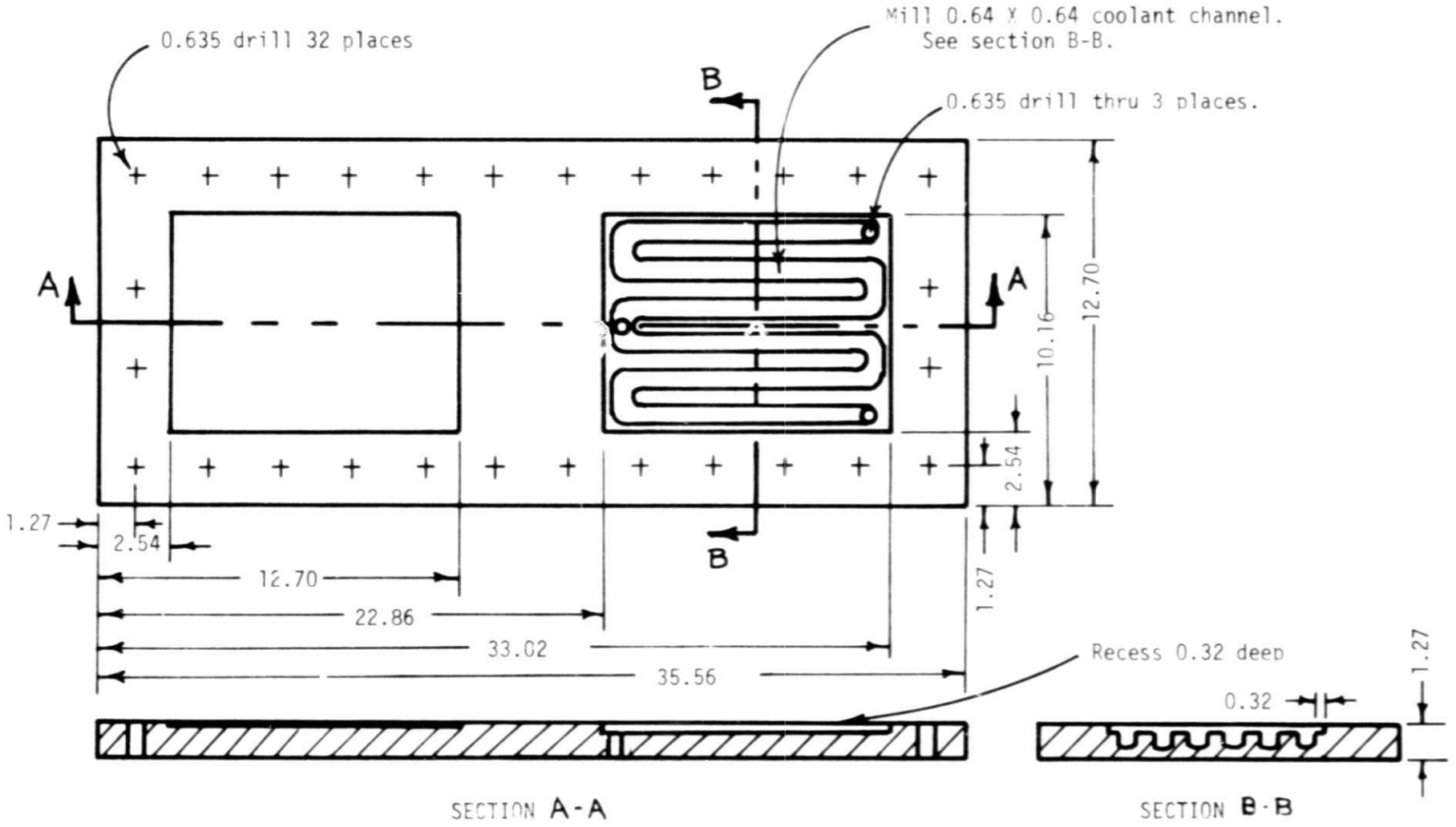

Figure 11. Lexan Base Plate. Dimensions in Centimeters.

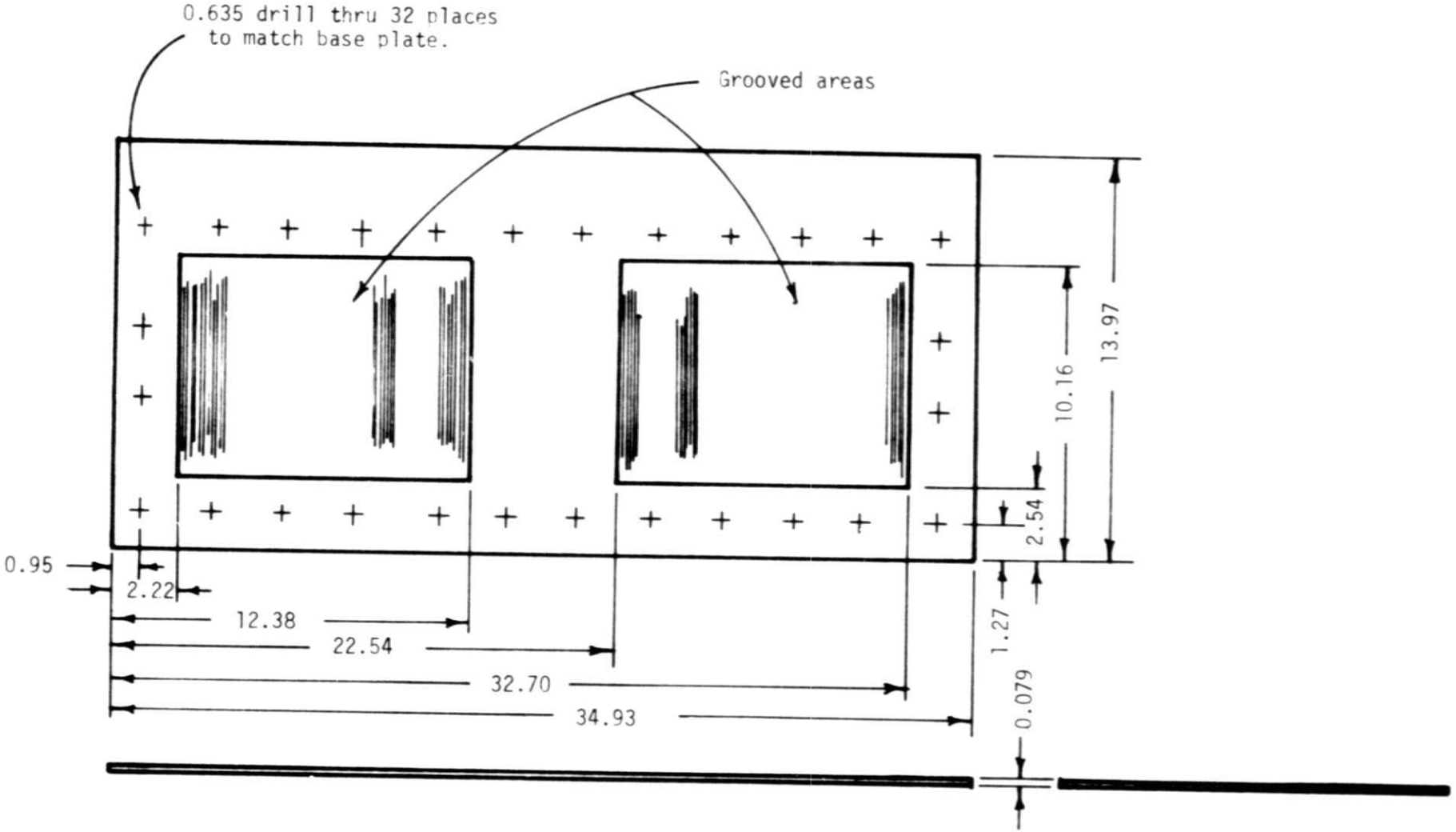

Figure 12. Aluminum Active Surface. Dimensions in Centimeters.

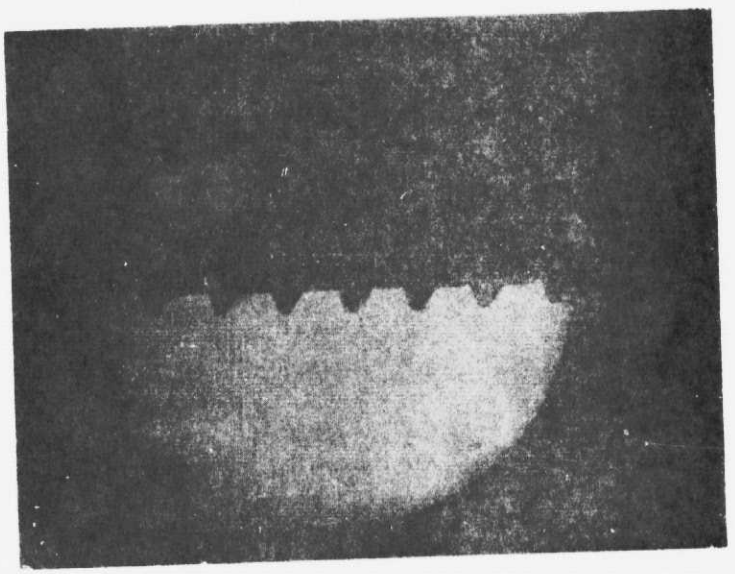

Figure 13. Groove Profiles.

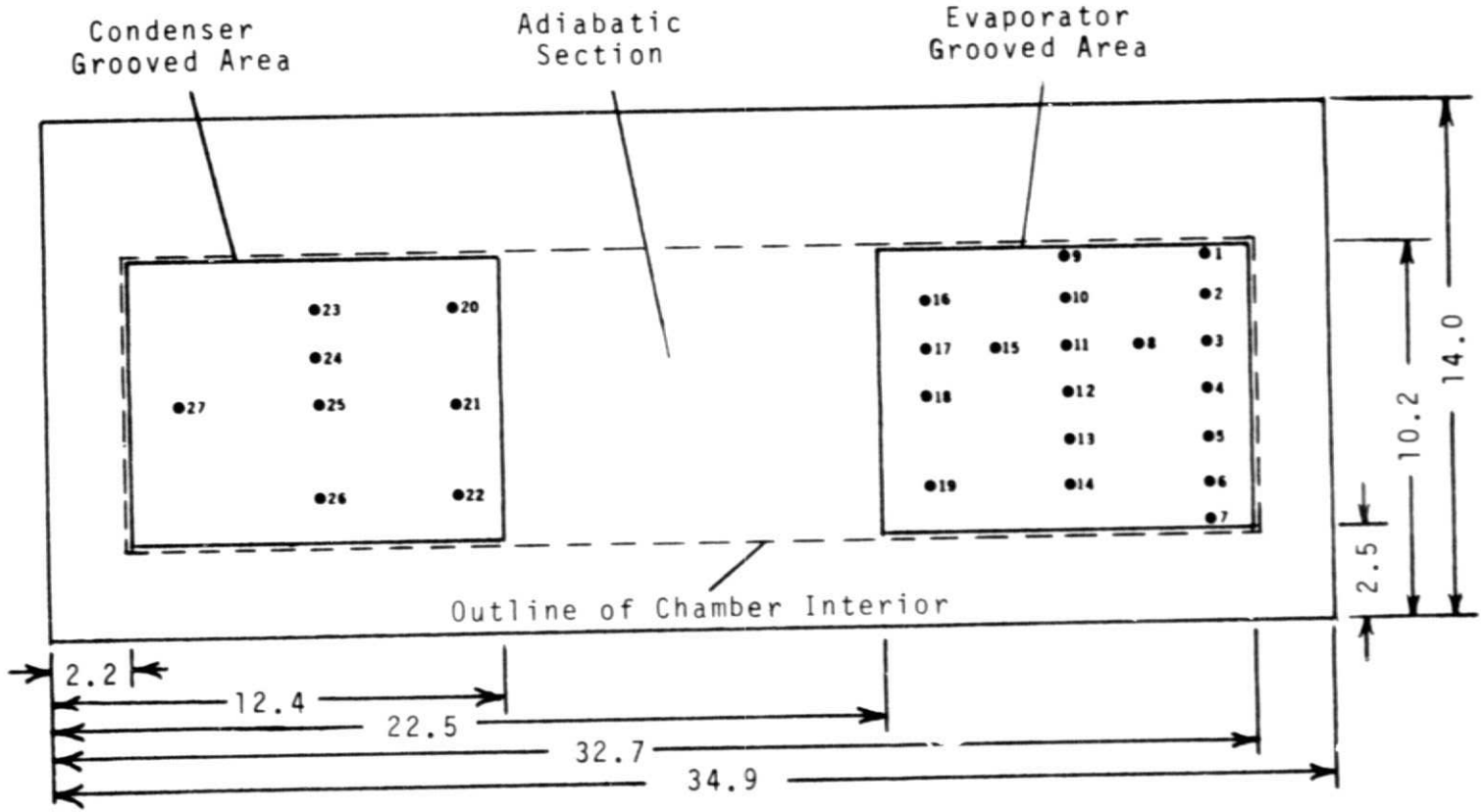

Figure 14. Heat Pipe Base Plate
With Thermocouple Locations (Dimensions in cm.)

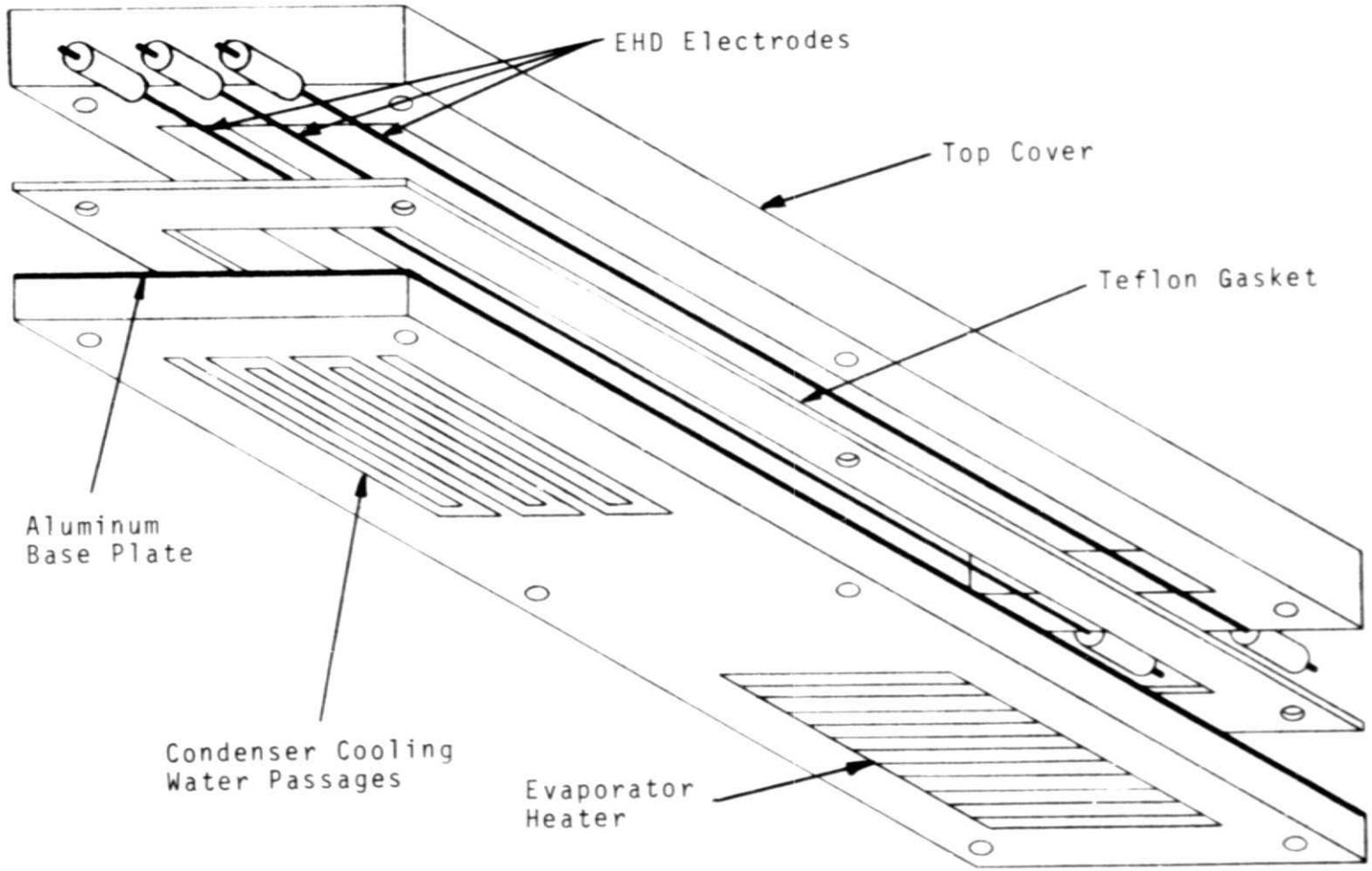

Figure 15. Exploded View of EHD Heat Pipe.

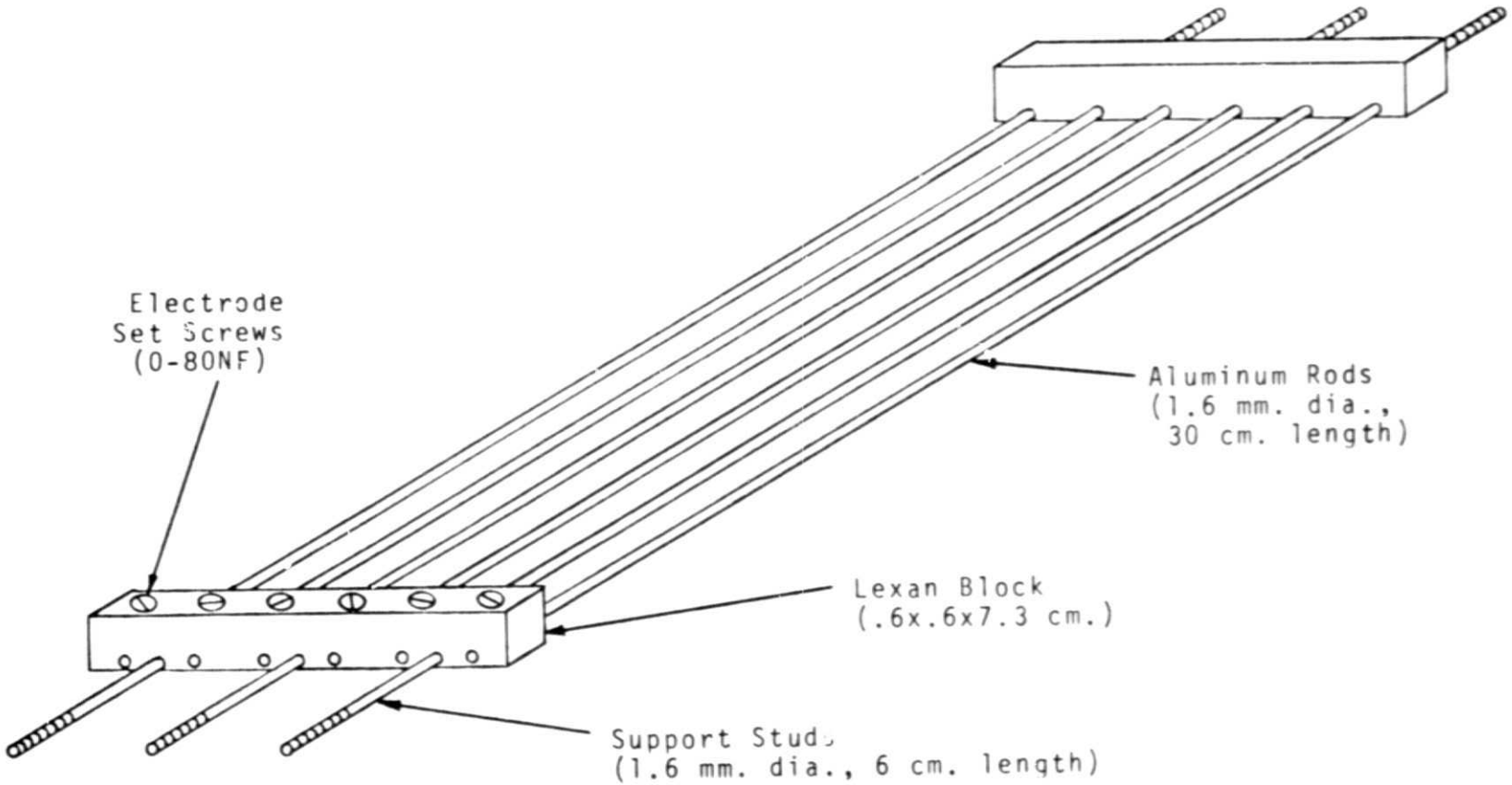

Figure 16. Six Electrode Adapter

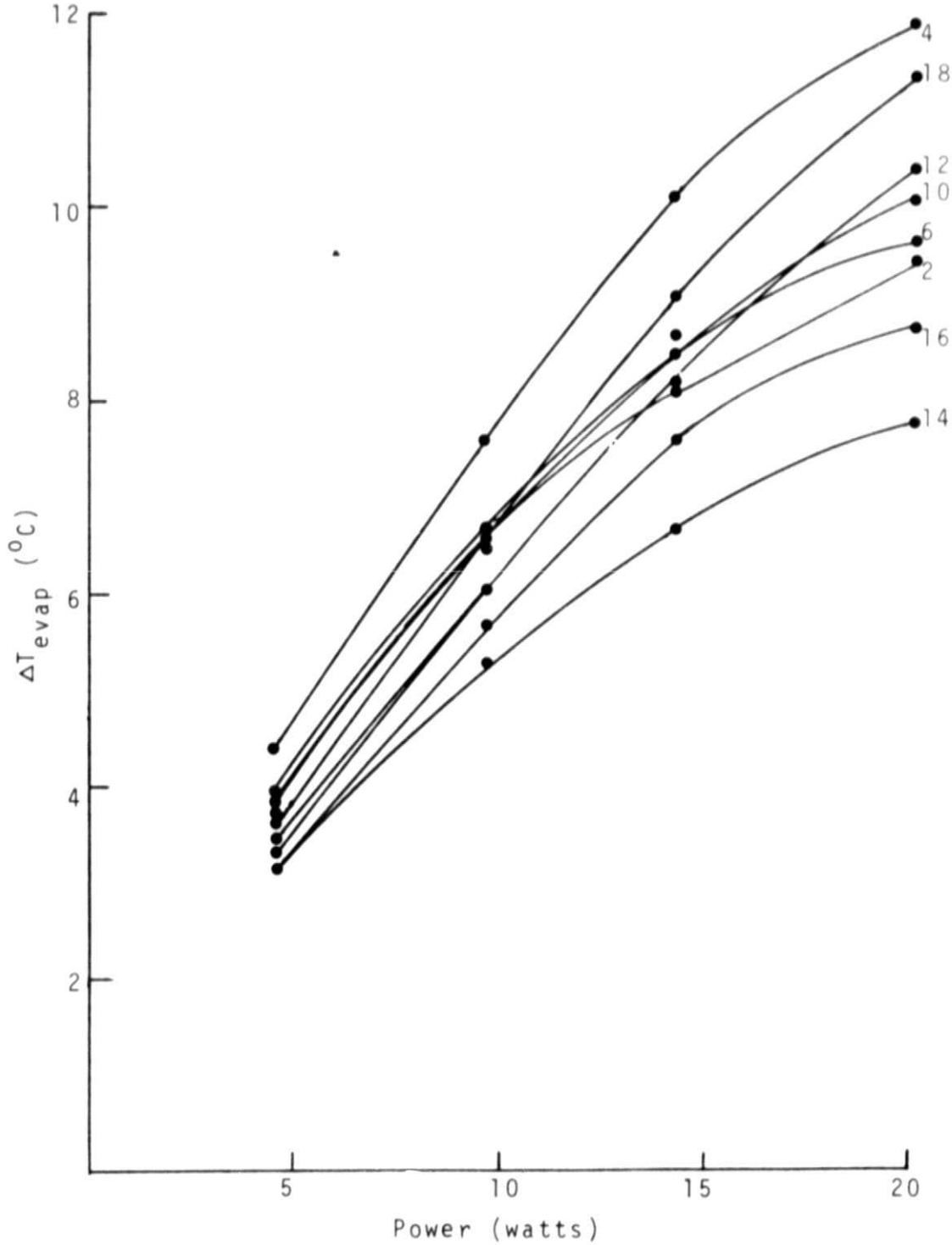

Figure 17. ΔT_{evap} vs. Power (0° tilt, no EHD)

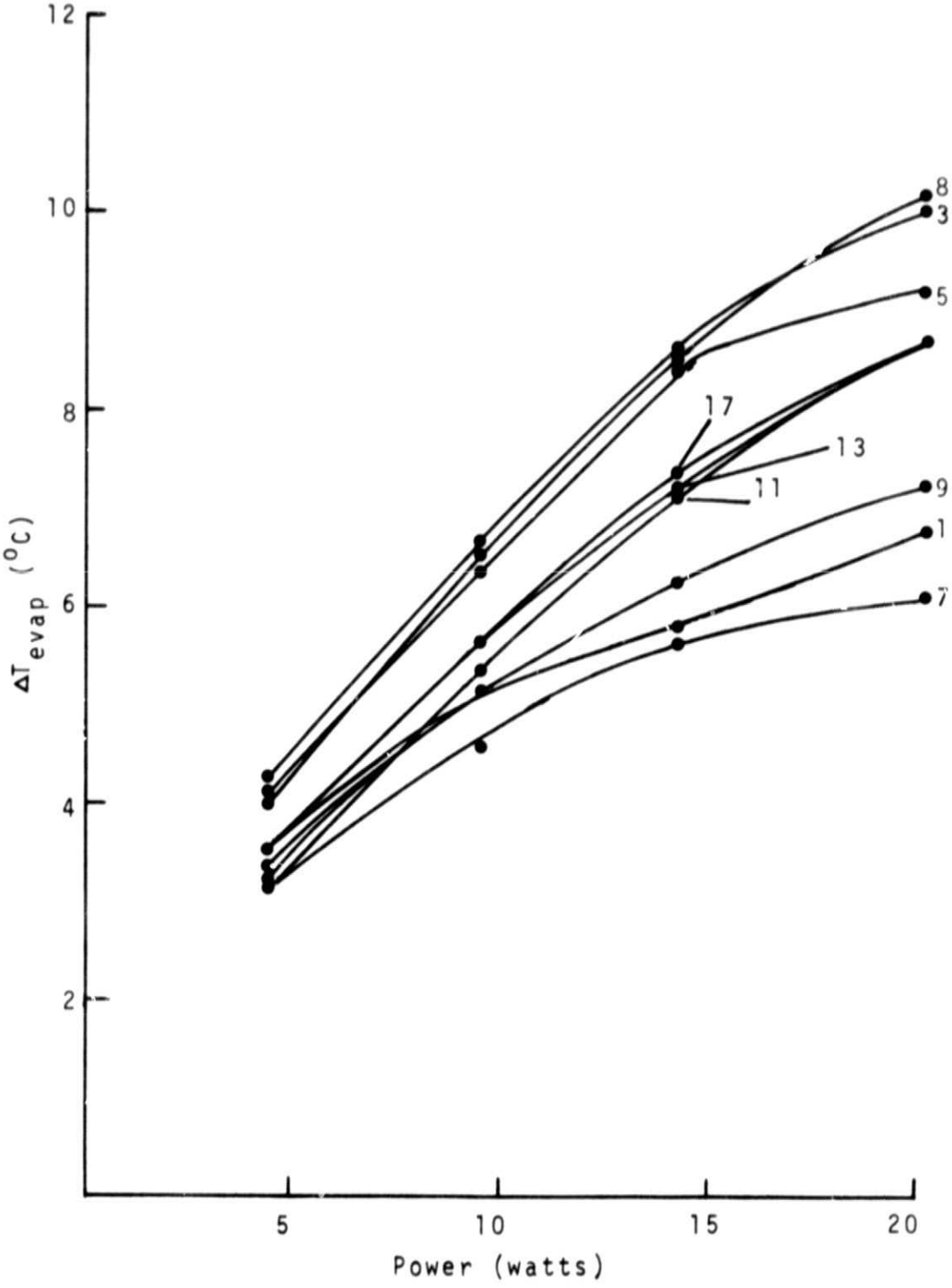

Figure 18. ΔT_{evap} vs. Power (0° tilt, no EHD)

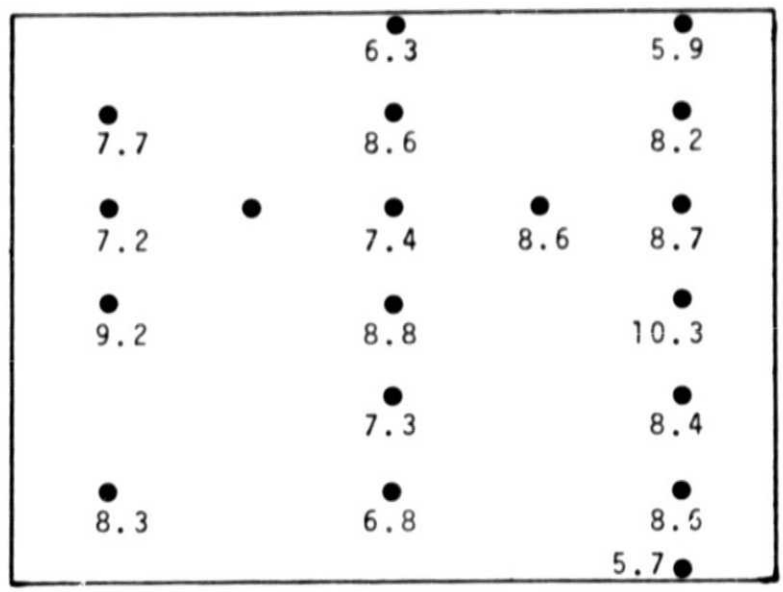

T_{vapor} = 30.7°C

Input Power = 14.3 watts

Figure 19. Distribution of ΔT_{evap} (°C) Over the Evaporator Surface

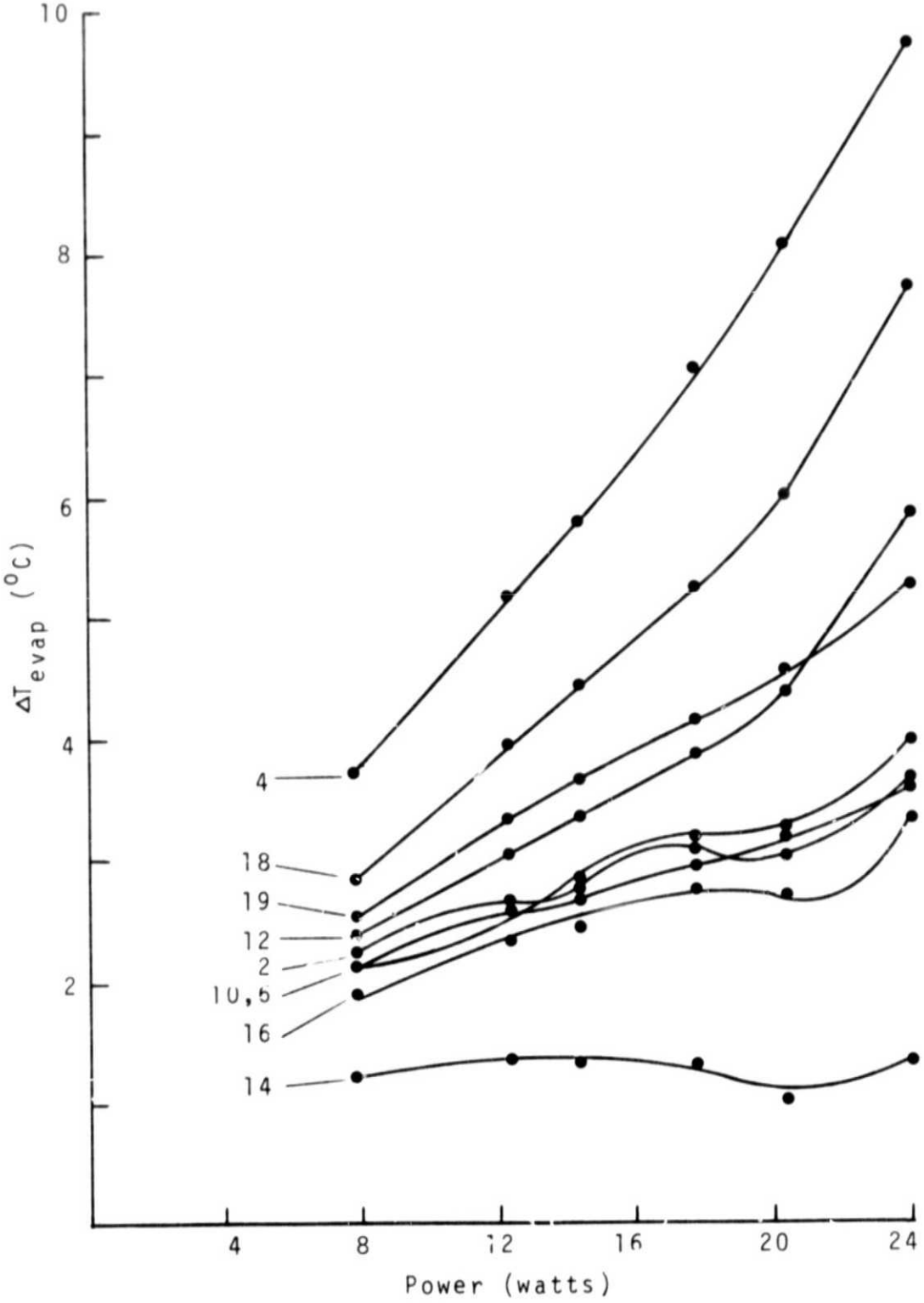

Figure 20. ΔT_{evap} vs. Power (5/26/74 data)

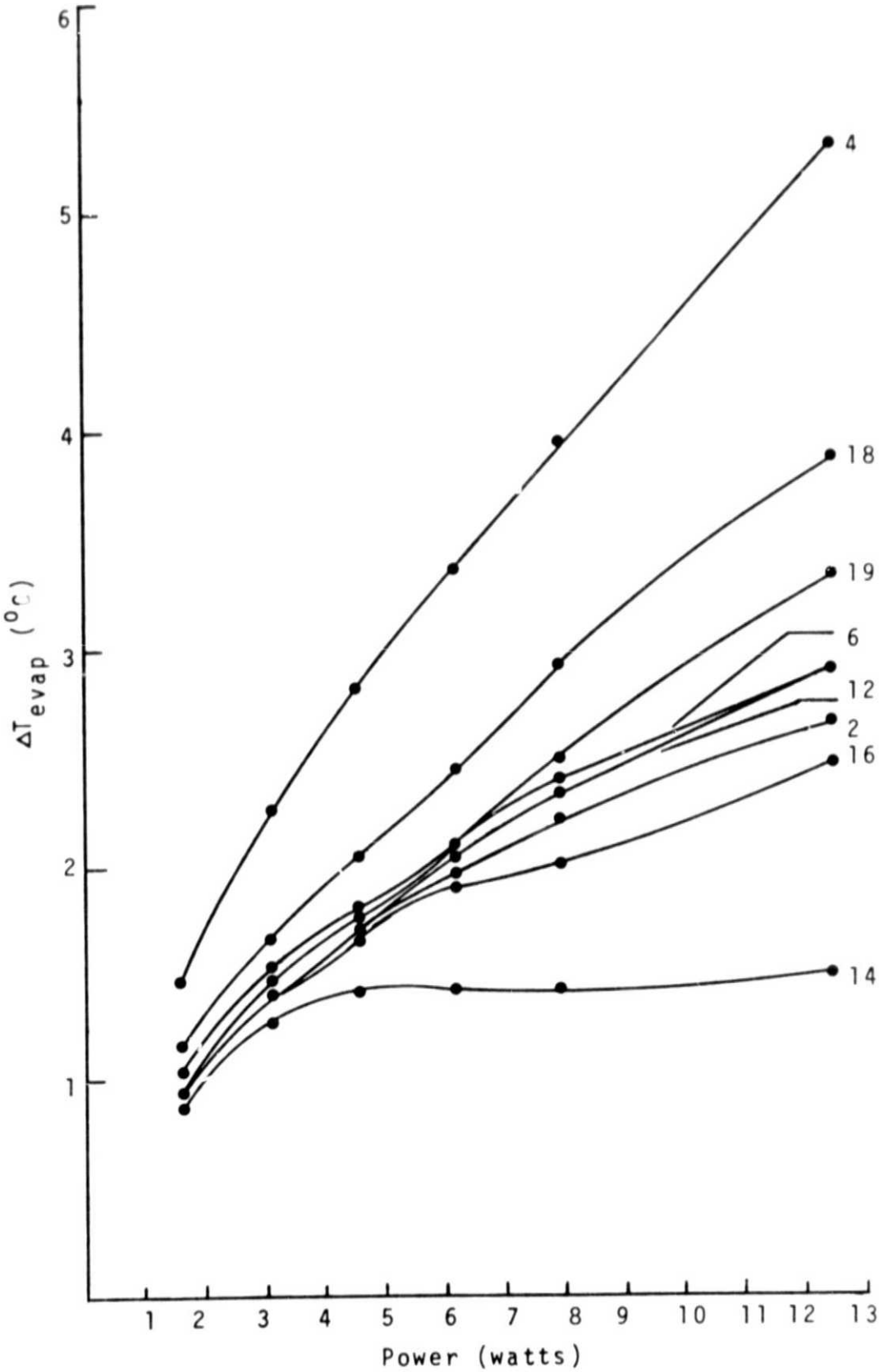

Figure 21. ΔT_{evap} vs. Power (Low Power Test)

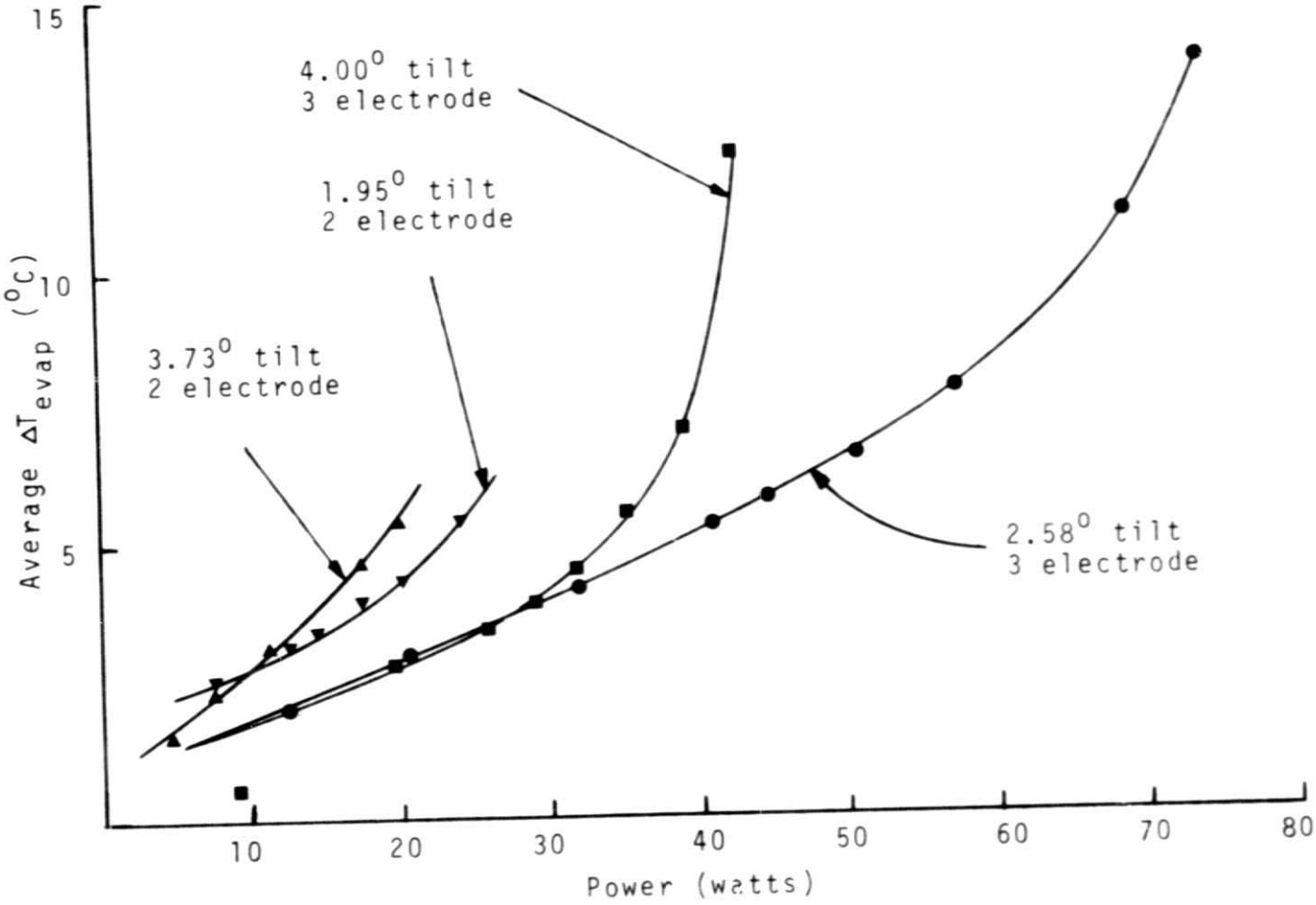

Figure 22. Average ΔT_{evap} vs. Power (.5mm. gap)

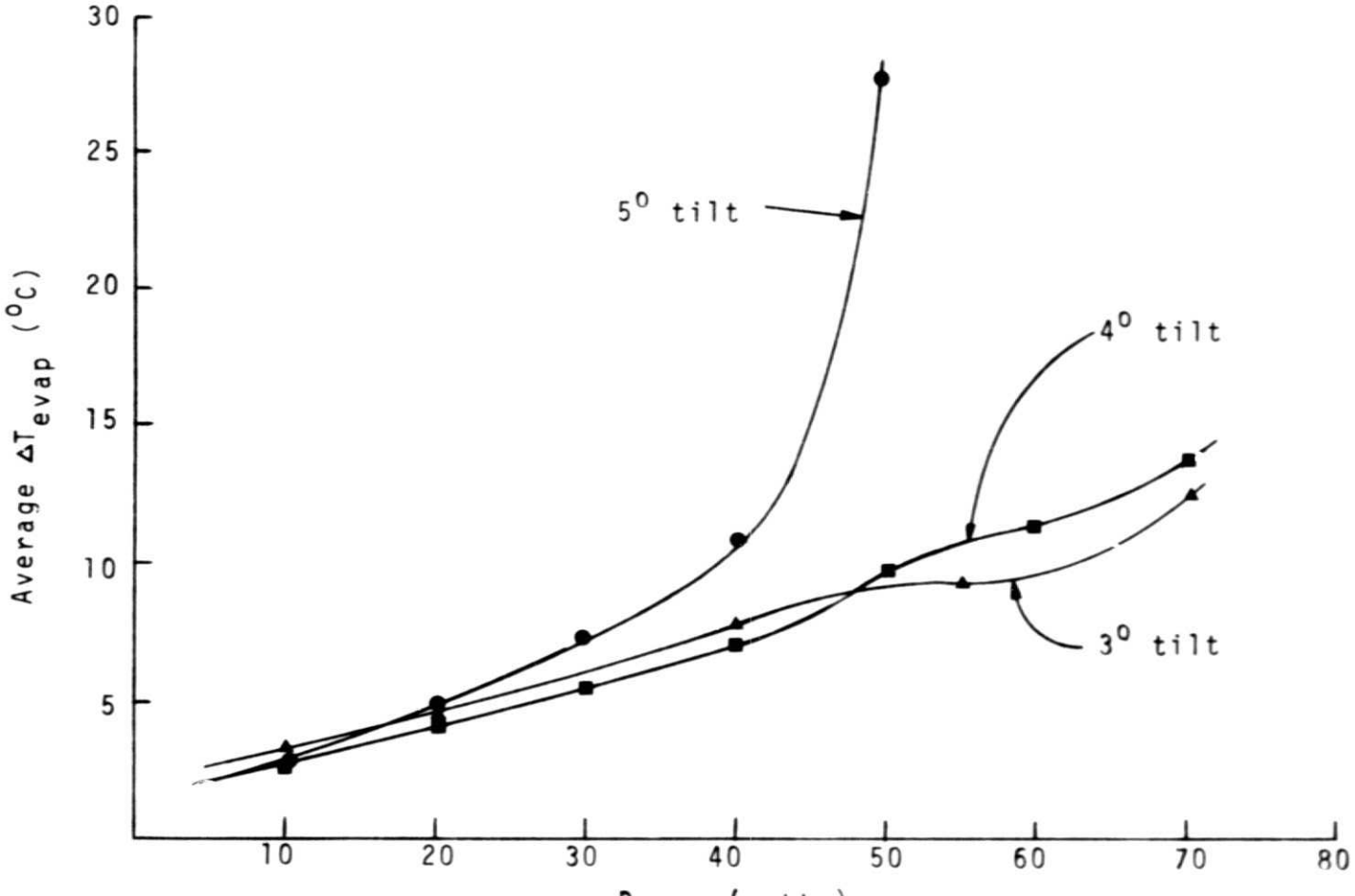

Figure 23. Average ΔT_{evap} vs. Power
(3 electrode, 1mm. gap)

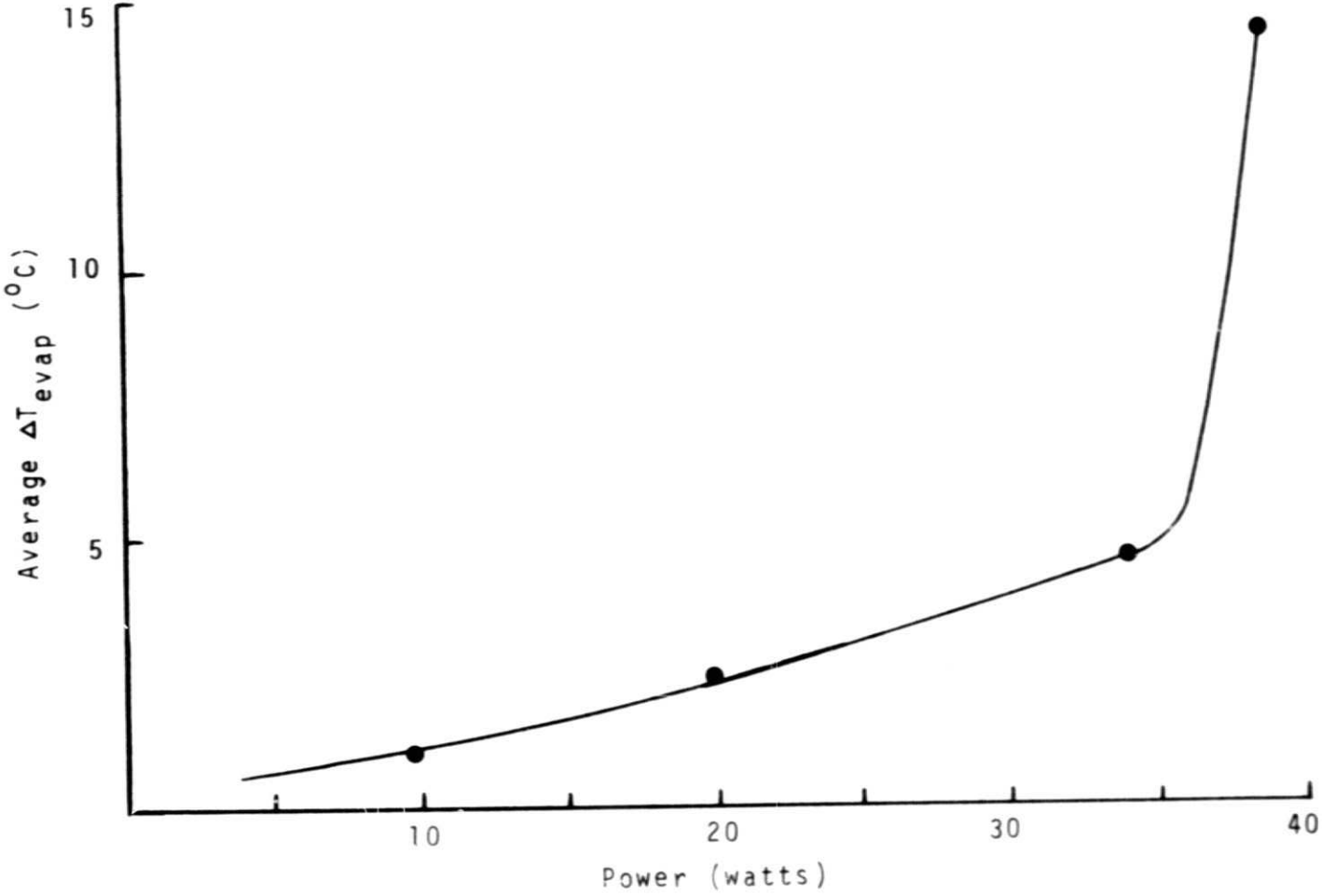

Figure 24. Average ΔT_{evap} vs. Power (6 electrode, 1mm. gap)